Stony Brook University

BMP-2 Gene Delivery using Electrospun Collagen/PLLA Scaffold with Surface Adsorbed Transfection Complexes for Bone Formation

A Dissertation Presented

by

Xia Zhao

to

The Graduate School

in Partial Fulfillment of the

Requirements

for the Degree of

Doctor of Philosophy

in

Biomedical Engineering

Stony Brook University

May 2015

Stony Brook University
The Graduate School

Xia Zhao

We, the dissertation committee for the above candidate for the
Doctor of Philosophy degree, hereby recommend
acceptance of this dissertation.

Dr. Michael Hadjiargyrou – Dissertation Advisor
Professor, Department of Biomedical Engineering

Dr. Emilia Entcheva - Chairperson of Defense
Professor, Department of Biomedical Engineering

Dr. Sanford Simon- Committee member of Defense
Professor, Department of Biomedical Engineering

Dr. Yizhi Meng-Committee member of Defense
Assistant professor, Department of Materials Science and Engineering

This dissertation is accepted by the Graduate School

Charles Taber
Dean of the Graduate School

Abstract of the Dissertation

BMP-2 Gene Delivery using Electrospun Collagen/PLLA Scaffold with Surface Adsorbed Transfection Complexes for Bone Formation

by

Xia Zhao

Doctor of Philosophy

in

Biomedical Engineering

Stony Brook University

2015

Bone tissue engineering provides an alternative to bone grafting. Our laboratory previously developed two different types of electrospun scaffolds for bone tissue engineering, including a DNA containing PLGA/PELA scaffold for delivering genes and a collagen/PLLA scaffold for delivering cells. For this dissertation research, we firstly fabricated a DNA containing PLGA/PELA electrospun scaffold using the same method as previously developed, with the intent of delivering osteogenic growth factor genes for bone regeneration. However, the scaffold shrunk severely after being submerged into aqueous environment and failed to achieve high transfection efficiency *in vitro*. Subsequently, we used the collagen/PLLA scaffold (originally developed for cell delivery) and modified our approach by surface immobilization of DNA/lipid complexes and showed superior transfection efficiency in Hela cells. Hence, BMP-2 gene delivery was performed using this collagen/PLLA scaffold with surface adsorbed transfection complexes on MC3T3 cells. Significant increase of mRNA level of BMP-2 expression

was observed after 3 days of transfection and as were other preosteoblast differentiation markers at the mRNA level by day 7. However, the BMP2 protein expression was not detected and augmentation of mineralization was not observed *in vitro* probably due to the cytotoxicity of the transfection reagent. In contrast, in an *in vivo* setting, the BMP2 transfection complex immobilized collagen/PLLA scaffold successfully transfected surrounding tissue with both mRNA level and protein level expression. In addition, the BMP2 transfection complex loaded scaffold successfully induced ectopic mineralization in mouse skeletal muscle. These results indicate that the surface adsorption strategy is a promising approach to immobilize gene delivery vehicles onto electrospun scaffolds for bone tissue engineering applications.

Table of Contents

List of Figures/Tables

List of Abbreviations

BMP	bone morphogenetic protein
PLA	poly-lactide
PEG	polyethylene glycol
PELA	PEG-PLA copolymer
PCL	poly(ε-caprolactone)
PLLA	poly-L-lactide
PGA	poly-glycolide
PLGA	poly lactide-co-glycolide
MSCs	mesenchymal stem cells
GFP	green fluorescent protein
OSX	osterix
RUNX2	runt-related transcription factor 2
COL1A1	type I collagen
αMEM	alpha modified minimum essential medium
qRT-PCR	Quantitative Real Time Reverse Transcriptase Polymerase Chain Reaction
SEM	Scanning Electron Microscopy
microCT	Micro-computed Tomography

Acknowledgments

I give heartfelt thanks to my advisor Dr. Michael Hadjiargyrou for all of his support and help during my PhD study. His expertise on research directed my study on the right track. He also respects students' ideas and gives a lot of flexibility on their study. He is always available when help is needed. He is magnanimous and patient to students' mistakes and shortcomings. His passion on science, diligence, his scientific attitude on research and his excellent writing skills are all worthy for our students to learn in life.

I am particularly grateful to Dr. David Komatsu for serving as my secondary advisor when Michael left the school. His help with providing laboratory space and materials, and his expertise on research assured the completion of my study.

Many thanks to my committee members: Dr. Sanford R. Simon, Dr. Emilia Entcheva, Dr. Yizhi Meng for their expertise on my proposal and dissertation.

I thank my colleagues: Dr. Cheng Liu, Dr. Jonathan Chiu, Dr. Robert Gersh, Dr. Hui Pan, Dr. Yen Kim Luu, Dr. Sardar Uddin, for their training on experimental skills and expertise on experimental designs. I also thank Dr. Long Bi for his direction on animal study.

I appreciate all the training and support from the Department of Biomedical engineering of Stony Brook University.

1. Introduction

1.1 Overview

Loss of bone resulting from trauma, infection and tumor resection and skeletal abnormalities is a worldwide problem severely affecting human health[1, 2]. Surgeons use autografts or allografts to repair major damage to bone from accidents or disease. An estimated 450,000 surgical bone grafts are performed each year[1]. However, autografts are limited by poor quality and quantity of bones that can be harvested. Other disadvantages include, donor site morbidity caused by additional surgical procedures for harvesting, risk of infection, hematoma formation and chronic pain[1-3]. Allografts have other limitations like transmission of diseases from donor to recipient or immunogenic reactions[3]. Bone tissue engineering, which aims to develop viable, clinically competitive approaches (e.g. scaffolds) for bone reconstruction, provides an alternative to tissue grafting[4]. It requires that the scaffold be porous and conducive to cell attachment and maintenance of viability and appropriate cell function. Such a scaffold can be coupled together with a rich source of stem cells, osteoprogenitor cells or even osteoblasts and selected osteoinductive growth factors[5]. In the last decade, various bone tissue engineering approaches have been extensively studied and hold great promise in treating bone tissue loss. However, to date, a vascularized mechanically competent osteoconductive/inductive construct remains elusive.

The overall goal of the proposed research is to develop an implantable device which combines gene therapy with a tissue engineering scaffold, for long-term

production of selected bone osteoinductive factors to treat bone tissue loss and/or enhance endogenous regeneration.

1.2 Current progress in bone tissue engineering

A successful bone tissue engineering construct usually requires three interdependent properties: 1) osteoconduction (extracellular matrix (ECM)/scaffold for adhesion, migration, proliferation, and differentiation of cells), 2) osteoinduction (bone morphogenetic proteins (BMPs) and other growth factors to induce osteogenesis), and 3) osteogenesis (stem cells and osteoprogenitor cells within the matrix/scaffold) to produce new bone [2, 6, 7].

1.2.1 Extracellular matrix/scaffold

The ECM provides mechanical support for the bone tissue. It is vital to native bone formation and maintenance. Artificial ECM/scaffold are usually generated for developing a successful tissue engineering strategy. Many materials and scaffolding procedures are being used to create artificial ECM. Table 1 lists the important factors needed to be considered in scaffold design[6].

Environment	Properties	Architecture	Material
In vivo vs in vitro	Biocompatibility	Porosity	Biomimetic material
Static culture vs dynamic culture	Osteogenesis	Pore size	Natural vs synthetic
Growth factors	Osteocompatibility	Surface area to volume ratio	Bioactive vs bioinert
Access to vasculature	Osteoinduction	Pore interconnectivity	Factor release
Temperature	Osteoconduction		Mechanical Strength
pH	Mechanical strength		
	Preformed vs injectable		
	Surface texture		
	Degradation rate		

Table 1. Factors needed to be considered in scaffold design [6].

The materials commonly used can be divided into several categories including metals, ceramics (i.e. β-Tricalcium Phosphate (β-TCP), hydroxyapatite, biphasic calcium phosphate (BCP), octacalcium phosphate (OCP), and calcium-sulfate, etc.), natural polymers (i.e. collagen, fibrin, gelatin, glysosaminoglycans (GAGs), and chitosan et al), synthetic polymers(poly(ε-caprolactone)(PCL), poly-L-lactide (PLLA), poly-glycolide (PGA), poly lactide-co-glycolide (PLGA), etc.) and composites of these

materials [8, 9]. One major disadvantage of metals and ceramics is their lack of degradability within a biological environment and their restricted processing capability. In contrast, polymers have great design flexibility and thus have received considerable attention and are more widely studied for bone tissue engineering applications [9].

Other than the diversity of materials, a number of different scaffolding methods were developed for preparing porous 3D polymeric scaffolds for bone tissue engineering. These techniques mainly include solvent casting and particulate leaching, gas foaming, emulsion freeze/drying, electrospinning, rapid prototyping, thermally induced phase separation and 3D printing etc. [9, 10] and currently are all being tested.

1.2.2 Osteoprogenitor cells within matrix/scaffold

In order to stimulate efficient bone regeneration, an adequate supply of cells (mesenchymal stem cells (MSCs) and osteoprogenitors) is critical. Enhanced repair of large bony defects in animals have been achieved by implanting scaffolds loaded with MSCs of diverse species [11-15]. Moreover, a few clinical trials were conducted with transplanted scaffolds containing human bone marrow-derived MSCs to treat large bone defects and obtained promising results [16, 17]. However, due to difficulties of the *ex vivo* enrichment, in addition to donor-dependent disadvantages regarding the bone forming capacity, further investigations are needed to fully realize the therapeutic applications of MSCs. Utilization of MSCs from sources other than bone marrow, such as peripheral blood [18], fat [19], muscle, traumatized muscle tissue after debridement [20], or even ESCs (embryonic stem cells) [21] are also under extensive investigation.

1.2.3 BMPs and other growth factors

A number of key molecules that regulate the complex bone regeneration process have been identified, including BMPs, platelet-derived growth factor (PDGF), transforming growth factor-β (TGF-β), insulin-like growth factors (IGFs), vascular endothelial growth factor (VEGF) and fibroblast growth factors (FGFs), just to name a few [22]. BMPs have been the most extensively studied among these molecules because of their potent osteoinductive properties. They act on the chemotaxis and mitogenesis of MSCs and other osteoprogenitor cells, and induce their differentiation to osteoblasts[23]. Since the discovery of BMPs, a number of animal and clinical trials have shown the safety and efficacy of their use as osteoinductive bone-graft substitutes for bone regeneration[2]. Further, with the use of recombinant DNA technology, rhBMP-2 (INFUSE, Medtronic) and rhBMP-7 (OP-1, Stryker) have also been commercially available for clinical use for over a decade now[24].

Despite extensive research and development of growth factor products for bone regeneration, the clinical application of these proteins is still limited by difficulties of controlled and sustained delivery. These soluble proteins have a very short half-life *in vivo* due to rapid diffusion and proteolytic degradation, leading to dosages that are far above physiological levels, thereby incurring higher costs[25]. In addition, problems of unwanted ectopic bone formation, bone resorption and heightened soft tissue reactivity were also reported[24].

1.3 Gene therapy in bone tissue engineering

Other than direct protein delivery, gene therapy is another promising approach for growth-factor delivery in the field of bone tissue engineering[25]. Instead of delivering proteins with their aforementioned disadvantages, gene therapy transfers genetic material into the target cells, allowing expression of bioactive factors from the cells themselves for a prolonged time. Gene therapy can be performed by either an *in vivo* or *ex vivo* strategy. The *in vivo* method delivers the desired gene directly into the target tissue; in contrast, the *ex vivo* technique requires the target cells to be harvested, expanded in culture, transfected and implanted back into the host[25].

Gene therapy approaches entail the use of either viral or non-viral vectors to deliver the therapeutic gene, or even naked DNA. Predominantly, viral vectors are used and include adenovirus, adeno-associated virus, herpes simplex virus, lentivirus and retroviruses. Viral vectors are extremely efficient at delivering the therapeutic gene and with high levels of infection, but have the disadvantages of immunogenicity, toxicity and mutagenicity[26]. On the other hand, non-viral vectors tend to be polymeric or lipid based, and in comparison to viral vectors, they are easy to manufacture and have low cost and low immunogenicity. However, their biggest disadvantage is their low transfection efficiency and this needs to be improved, especially for *in vivo* applications [27].

Using a gene therapy approach, the delivery of growth factor, particularly BMPs, for bone regeneration has already produced promising results in animal studies [28, 29]. Lieberman et al used an adenovirus vector to deliver BMP-2 into MSCs and these cells successfully healed large segmental femoral defects in nude rats [30]. In another study,

periosteal cells transduced retrovirally with BMP-7 were seeded onto PGA matrices and implanted into bone defect site. This approach successfully enhanced the repair of critical-size rabbit cranial defects[31]. However, these studies were accomplished using viral vectors, despite their disadvantages described above. To circumvent this, our laboratory is currently developing non-viral approaches to deliver genes for bone regeneration.

1.4 Current progress of bone tissue engineering study in our laboratory

For over a decade, our laboratory has utilized electrospinning to fabricate polymeric scaffolds for cell, drug and gene delivery [32-35]. Electrospinning is a versatile technique used to generate tissue engineering scaffolds due to its ability to produce micro and nanofibers from polymeric solutions or melts[36]. By applying a high electric field between a syringe tip and a grounded collector, the polymer solution or melt is slowly extruded out of the syringe tip and is collected typically on a rotating drum. Specifically, when the force surpasses the surface tension of the polymer solution at a critical voltage, an unstable, electrically charged jet is pulled out from the syringe tip and falls onto the collector. During this extrusion process, almost all of the solvent is evaporated, and a single continuous fiber is formed on top of the collector. Over time, the collected fiber eventually accumulates into a nonwoven fibrous sheet[36] (Figure 1).

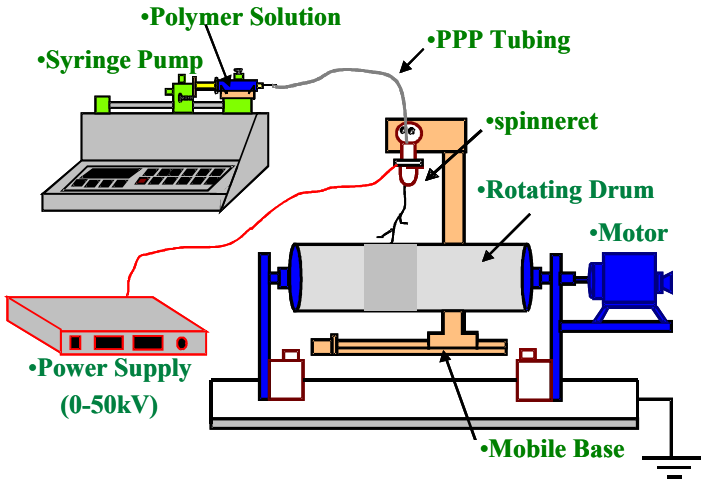

Figure 1 Electrospinning apparatus in creating nonwoven, nanofibrous scaffolds[37].

Such electrospun scaffolds are of great interest and widely studied for tissue engineering applications due to their various advantages in comparison to other types of scaffolds; first, they can mimic the nanoscale structure of the ECM; second, their nonwoven, nanofibrous nature constructed from biodegradable polymers leads to high porosity, high surface to volume ratio and controllable degradation; third, they are simple and easy to fabricate and bioactive molecules can be easily incorporated, and fourth, by fine-tuning a number of factors (e.g. polymer solution composition, surface tension, electric field strength), it is possible to precisely control the composition and morphology of the scaffolds for desired biocompatibility, biodegradability and functionality[36].

A number of natural and synthetic materials have been electrospun into fibrous meshes for bone tissue engineering applications, including collagen[38], chitosan[39], silk fibroin[40, 41], poly(L-lactic acid) (PLLA)[42], poly(lactide-co-glycolide acid) (PLGA)[43], poly(caprolactone) (PCL)[44], and blends of these materials[45-47]. Our laboratory has

also reported on previous studies using PLGA[33], PLLA and collagen[37] to develop electrospun bone tissue engineering scaffolds. Specifically, PLGA has been used as a base polymer, due to its excellent biocompatibility and biodegradability as well as its ability to be easily modified to combine with natural polymers, including extracellular proteins, growth factors or even drugs in order to provide different functionality to the scaffolds [48-50]. PLLA also demonstrated good biocompatibility, superior material properties, and slow degradation rate, which are all favorable for bone applications [35, 51-58]. For example, a PLLA electrospun scaffold retained less than 40% of original intensity after 4 weeks of subcutaneous implantation as detected by gas permeation chromatography [59]. An electrospun PLLA/PCL mixture scaffold demonstrated about 50% of weight loss after 21 days of degradation in vitro [60]. Futher, modulation of the material composition and parameters of electrospinning can also alter the degradation property of the scaffold. The ideal optimal material/mechanical properties of the electrospun scaffold should match those of the bone tissue that needs to be regenerated. To achieve this, incorporation of hydroxyapatite (HA) and creation of fiber alignment improve the mechanical properties of electrospun scaffolds [61, 62]. Moreover, it was reported that low M.W. PLLA (M.W. 20000) could enhance the differentiation of MC3T3-E1 cells [58]. Type I Collagen is also another candidate molecule for scaffold incorporation as it is the main component of mammalian connective tissue, accounting for approximately 90% of bone ECM protein content [63]. Furthermore, collagen contains RGD sequences, which mediate reciprocal interactions between ECM molecules and intracellular cytoskeleton via integrins [64]. However, collagen's poor bulk properties and high expense (when

purchased in its pure form) limit its utility as the sole component in tissue engineering scaffolds, and thus, it is usually used together with PLGA or PLLA base polymers [47].

Previously, our laboratory fabricated two types of 3D non-woven highly porous electrospun scaffolds for the application of bone tissue engineering: one is composed of PLGA/PLA-PEG-PLA (LEL) and DNA for osteoinductive gene delivery purpose[33]; the other is composed of PLLA and small amount of collagen for osteogenic cell delivery purpose[34]. The PLGA/LEL/DNA scaffold was the first electrospun tissue engineering scaffold that demonstrated successful plasmid DNA incorporation, release and *in vitro* delivery of bioactive DNA capable of transfection and expression. Specifically, the released DNA from the scaffold exhibited enhanced transfection efficiency in comparison to equivalent amounts of naked plasmid DNA. However, the transfection efficiency of the released DNA was lower than the one further complexed with transfection reagent Fugene 6 (~4%), and much lower than the same amount of original plasmid complexed with Fugene 6 (~20%). [33]. Based on these results, it was hypothesized that the transfection efficiency of the scaffold could be enhanced by seeding cells directly onto it. In addition, direct seeding of cells on this scaffold can enable us to determine the cell compatibility property of the scaffold. Hence, the first specific aim of this study further investigated the *in vitro* transfection efficiency and cell compatibility of this type of electrospun scaffold.

Our laboratory was also the first one to develop collagen incorporated PLLA electrospun scaffolds for the enhancement of preosteoblast differentiation. The collagen (<1 wt %) containing PLLA scaffolds developed supported robust cell attachment, sustained cell proliferation and differentiation, and greatly enhanced cell penetration in

comparison with pure PLLA scaffold[34]. The superior cell compatibility of the collagen/PLLA scaffold encouraged us to further explore the feasibility of modifying this scaffold, so that it can serve as a gene delivery system as well, for the ultimate goal of generating an effective bone tissue engineering construct. Therefore, in the second and the third specific aims of this study, the collagen/PLLA scaffold was modified by surface adsorption of transfection complexes and rhBMP2 gene delivery efficacy was investigated using this modified scaffold *in vitro* and *in vivo*, respectively.

1.5 Specific Aims & Hypotheses

Specific Aim 1: Development, characterization and evaluation of the *in vitro* transfection efficiency of DNA containing PLGA/PEG-PLA composite electrospun scaffold.

Hypothesis 1: DNA incorporated in a PLGA/PEG-PLA composite electrospun scaffold will successfully be released and will retain its bioactivity.

Hypothesis 2: Cells plated onto the DNA containing PLGA/PEG-PLA composite electrospun scaffold will be successfully transfected.

Specific Aim 2: Evaluating the ability of an electrospun collagen/PLLA scaffold with surface adsorbed BMP-2 DNA transfection complexes to deliver BMP-2 DNA and stimulate preosteoblast differentiation *in vitro*.

Hypothesis: Preosteoblast cells plated onto the electrospun collagen/PLLA scaffold with surface adsorbed BMP-2 DNA transfection complexes will be successfully transfected and undergo differentiation.

Specific Aim 3: Assessing the ability of the electrospun collagen/PLLA scaffold with surface adsorbed transfection complexes to deliver BMP-2 DNA and stimulate ectopic bone formation *in vivo*.

Hypothesis: The implanted electrospun collagen/PLLA scaffold with surface adsorbed BMP-2 DNA transfection complexes will be successfully delivered into surrounding tissue and induce ectopic bone formation.

2. Specific aim 1

Development, characterization and evaluation of the *in vitro* transfection efficiency of DNA containing PLGA/PEG-PLA composite electrospun scaffold.

In this specific aim, a PLGA/PEG-PLA composite electrospun scaffold was fabricated using the same method developed by our laboratory previously[33]. The main difference of this scaffold from the previous developed is the use of the diblock copolymer PEG-PLA instead of the triblock copolymer PLA-PEG-PLA. DNA release study was performed and the integrity of the released DNA was analyzed using gel electrophoresis and *in vitro* cell transfection study. Finally, cells were plated directly on the scaffold for testing the cell compatibility and the *in vitro* transfection capability of the scaffold.

2.1 Materials and Methods

2.1.1 Materials

75:25 PLGA was purchased from Birmingham Polymers (Birmingham, AL, USA, Cat. No.A144-75), with an inherent viscosity of 0.69dL/g in $CHCl_3$. PEG-PLA (5K-5K) diblock copolymer (intrinsic viscosity: 0.55dL/g in CHCl3) was kindly provided by Dr. Benjamin Chu's (Department of Chemistry, Stony Brook University) laboratory. MC3T3-E1 cells were purchased from ATCC (Manassas, VA, USA). GFP containing plasmid pECFP-C1 (4.7kb) was purchased from Clontech (Mountain View, CA, USA) and amplified through E. coli culture using a Qiagen (Valencia, CA, USA) Giga Prep kit. Picogreen DNA reagent was obtained from Molecular Probes (Eugene, OR, USA).

Nuclear fast red reagent is obtained from ScyTek Laboratories (Logan, Utah, USA). Fugene HD transfection reagent was purchased from Roche Applied Science (Indianapolis, IN, USA).

2.1.2 Electrospinning and morphology of the electrospun scaffolds

The general method for scaffold fabrication was followed as previously described by our laboratory[33]. PEG-PLA block copolymer (0.12g) was dissolved in 2.68g N, N-dimethyl formamide, to which 200µl GFP plasmid solution (5mg/ml, dissolved in water) were added. The solution was stirred to stabilize for half an hour, after which 1.2g PLGA (LA/GA 75:25) was slowly added to generate a 33% w/w polymer solution with the mass ratio of PEG-PLA block copolymer to PLGA 1:10. After transferring the polymer solution to a 5ml syringe fitted with a metal spinneret via a tubing, the syringe and the spinneret was set up in the electrospinning apparatus. The scaffold was electrospun at about 22kV with a solution flow rate of 30µl/min. And the distance between the spinneret and the rotating collection drum (covered with aluminum foil) was fixed at ~15cm. Scaffold without any DNA was fabricated and served as a control. Following electrospinning, the scaffolds were peeled off the aluminum foil and then cut into 1.5×1.0cm^2 sections.

The morphology of the scaffolds was studied using scanning electronic microscopy (SEM) by coating with gold and visualized by a LEO 1550 Field Emission SEM at an acceleration voltage of 10kV. The porosity of each membrane was estimated by using

porosity=$(1-\rho/\rho_0)\times100\%$[65], where ρ is the density of electrospun scaffold and ρ_0 is the density of PLGA. To calculate the ρ of the scaffolds, three 1.0×1.0 cm^2 sections were randomly cut from each scaffold, and then the weight, area and thickness of each section were measured. The average ρ of the three sections were taken as the final ρ for each scaffold.

2.1.3 DNA release assay

The electrospun scaffold was cut into 1.5×1.0cm^2 sections (n = 6), and each section was incubated individually in an Eppendorf tube containing1ml TE buffer at 37°C. At 2, 24, 48, 72, 96 and 120hr, scaffold sections were taken out and transferred to tubes containing fresh buffer and the collected release samples were stored at -20°C until the end of the assay. The amount of DNA released into TE buffer was quantified using PicoGreen Assay, which uses a fluorescent dye to stain double stranded DNA only. The DNA solution was excited at 485nm and the emitted fluorescence was measured at 530nm using a microplate reader (CytoFluor Series 4000, Perseptive Biosystems).

2.1.4 Gel electrophoresis

The structural integrity of the released DNA was determined by 0.8% agarose gel electrophoresis and visualized by ethidium bromide staining. The release samples from 1.5×1.0 cm^2 scaffold sections (n = 6) collected at 2 hours, day 1, day 3 and day 5 of release were pooled and precipitated using ethanol, and then dissolved in 10μl of water. 5μl of the precipitated DNA samples were loaded into a gel.

2.1.5 Cell culture and released DNA bioactivity

MC3T3-E1 cells were cultured in α-MEM supplemented with 10% BCS and 1% penicillin-streptomycin at 37ºC, 5%CO_2 and 95% humidity. 1×10^5 MC3T3 cells were plated on a 24-well plate one day prior to transfection. On the day of transfection, following manufacture's protocol, 2μg of original GFP plasmid or released GFP plasmid were dissolved in 94 μl of water and then 6 μl of Fugene HD transfection reagent was added to the DNA solution to make 100μl lipid/DNA complexes. The mixture was vortexed for 1 second immediately after the addition of the transfection reagent, then incubated in room temperature for 15 minutes. 25 μl of the complexes were added to each well of cells in the 24-well plate. For control groups, 2μg of naked original or released GFP was added directly into the 24-well plate. 3 days after transfection, the cells were photographed using a Zeiss microscope (Axiovert200), then treated with trypsin and resuspended in 500 μl of medium for FACS sorting to determine the transfection efficiency.

2.1.6 Cell behavior on the PLGA/PELA scaffold

DNA containing scaffold and control scaffold were cut into $1.0\times1.0cm^2$ scaffold sections and placed on the bottom of a 24-well plate. 1×10^5 cells were suspended in 30 μl of medium and carefully pipetted onto each $1.0\times1.0cm^2$ scaffold section. The droplet of cells on the scaffold was incubated in an incubator for 1 hour and then 500μl of medium was added into each well. After 3 days, the scaffold sections were taken out of the plate, fixed with 4 % paraformaldehyde and stained with nuclear fast red reagent.

Subsequently, the stained scaffold sections were embedded into OCT embedding medium and cut into 8 μm sections and photographed using a Zeiss microscope.

2.1.7 Transfection efficiency of the scaffold

Seven different test groups were performed to compare transfection efficiency as listed below.

Group 1: no GFP DNA scaffold only (scaffold only).

Group 2: no GFP DNA scaffold with transfection reagent Fugene HD supplement in cell culture medium (scaffold+Fugene HD).

Group 3: no GFP DNA scaffold with GFP plasmid supplemented in cell culture medium (scaffold+GFP).

Group 4: no GFP DNA scaffold with GFP plasmid/Fugene HD complexes supplemented in cell culture medium (scaffold+GFP/Fugene HD complexes).

Group 5: GFP DNA containing scaffold only (GFP scaffold).

Group 6: GFP DNA containing scaffold with Fugene HD reagent supplemented in cell culture medium (GFP scaffold+ Fugene HD).

Group 7: GFP DNA containing scaffold with additional GFP plasmid/Fugene HD complexes supplemented in cell culture medium (GFP scaffold+GFP/Fugene HD complexes).

For group 1 & 5, the same procedure of cell seeding was utilized as the above section (4.1.1.5). For group 2 & 6, 3, 4 & 7, an additional 1.5 μl Fugene HD reagent, 2μg of GFP plasmid DNA and 25μl of the GFP plasmid DNA/lipid complexes were added to each well, respectively, after the procedure of group 1 & 5. For evaluation of

transfection efficiency, cells were trypsinized for 5 min and resuspended in 500 µl of medium for FACS analysis.

2.1.8 Statistics

A one-way ANOVA coupled with a posthoc test was used to determine significant differences between the various groups in the transfection analysis.

2.2 Results

2.2.1 Fabrication and morphology of the scaffolds

The size of the scaffolds following electrospinning measured ~30×13cm. The thickness of the GFP DNA containing scaffold and the no DNA scaffold was 0.328±0.023mm and 0.305±0.019mm, respectively. Based on this size, and the starting amount of DNA, we calculated that the amount of DNA contained in a 1.5×1.0cm^2 scaffold to be about 3µg. SEM analyses showed that the general appearance of the DNA containing scaffold (Fig. 1a) was identical to that of the control scaffold without any DNA (Fig. 1b). Both scaffolds had a porous morphology with the fiber diameter around micron size. The porosity of the GFP DNA containing scaffold and the no DNA scaffold was ~80.5% and ~82.3%, respectively. The two scaffolds were both observed uniform without any "melts" or drops shown on them.

2.2.2 DNA release profile

We performed a release study over a maximum of 5 days. Similar to our previous study[33], a burst release was observed with ~60% of released DNA in the first 24 hours

followed by a steep decrease that occurred over time. Collectively, ~70% of plasmid DNA was released over 5 days, corresponding to about 2.2μg from each 1.5×1.0cm^2 scaffold section (Fig. 2).

2.2.3 Integrity of the released DNA

Following successful demonstration of DNA release from the scaffold, the integrity of the released GFP DNA plasmid was verified using gel electrophoresis. Results from this analysis showed that the migration of the released DNA (Fig. 3) appeared different than the control plasmid (unincorporated DNA). The lower band of each release sample migrated slower than the control plasmid DNA, but the top band of each sample was at the same position as the control. There was also some released DNA that remained in the loading well of the gel. The intensity of bands in lane 4 is much higher than other lanes, which is consistent with the release data showing maximum release occurred at day 1. As there was no "smear" (indicative of degraded DNA) observed in any of the released DNA samples, the results indicate that the released DNA was structurally intact.

2.2.4 Bioactivity of released DNA

Next, we wanted to investigate whether the released DNA retained its bioactivity, in the context of GFP expression in MC3T3 cells. The released GFP DNA plasmid preserved its expression capability (Fig. 4), although the transfection efficiency of DNA/Fugene HD complexes decreased from 50% to 14% (Fig. 5). The transfection efficiency of released GFP only, released GFP complexed with Fugene HD, original

GFP only; original GFP complexed with Fugene HD and cells only with no DNA is 0.045±0.070, 14.1±1.1, 0.013±0.010, 50.1±2.7, and 0.028±0.028, respectively. Group 2 and 4 have significant difference with each other and group 1, 3 and 5 ($p<0.001$), respectively. There is no significant difference between group 1, 3 and 5 ($p>0.05$).

2.2.5 Cell behavior on the scaffold

Cells plated onto the scaffold were only located on the surface of the scaffold and didn't infiltrate into it over 3 days (Fig. 6). Cells seeded on the scaffold were small (~1μm and even smaller than the fiber diameter) and round, meaning the viability of the cells growing on the scaffold was very low. In addition, the morphology of the scaffold significantly changed and the porosity dramatically decreased when used in the culture conditions. The control scaffold and the cells seeded on it had the same change and morphology and thus was not shown.

2.2.6 Transfection efficiency of the scaffold

The transfection efficiency of cells plated directly on the GFP containing scaffold was evaluated and compared to those on no GFP scaffold and other transfection approaches: group 1: scaffold only, group 2: scaffold+Fugene HD, group 3: scaffold+GFP, group 4: scaffold+GFP/Fugene HD complexes, group 5: GFP scaffold only, group 6: GFP scaffold+Fugene HD, group 7: GFP scaffold+GFP/Fugene HD complexes. The transfection efficiency of each group (1-7) is 0.22%, 0.03%, 0.28%, 2.08%, 0.37%, 0.57% and 2.85%, respectively. Group 4 (scaffold+GFP/Fugene HD complexes) and 7 (GFP scaffold+GFP plasmid/Fugene HD complexes) have significant

difference with group 1 (scaffold only), 2 (scaffold+Fugene HD), 3 (scaffold+GFP), 5 (GFP scaffold+GFP) and 6 (GFP scaffold+Fugene HD), respectively ($p<0.01$), but do not have significant difference between each other ($p>0.05$). There is also no significant difference between any two of Group 1(scaffold only), 2 (scaffold+Fugene HD), 3 (scaffold+GFP), 5 (GFP scaffold+GFP) and 6 (GFP scaffold+Fugene HD) ($p>0.05$). The overall transfection efficiency of the PLGA/PELA scaffold is lower than 3%, despite using the additional lipid/DNA complexes or not. But with the complexes (group 4(scaffold+GFP/Fugene HD complexes) & 7 (GFP scaffold+GFP plasmid/Fugene HD complexes)), the transfection efficiency is significantly higher than other groups.

2.3 Discussion

The electrospun PLGA/PELA scaffold with or without GFP plasmid had a porous morphology and a fiber diameter about a micron, similar to the DNA containing PLGA/LEL scaffold fabricated by our laboratory previously[33]. But when submerged into TE buffer or cell culture medium at 37°C, the scaffold shrunk to ~1/3 of its original size with much smaller pore sizes and much bigger fiber diameter as shown by Figure 6. The shrinkage of electrospun scaffolds in aqueous environments and the change of pore size are very common events and have been widely reported [65, 66]. To achieve a successful bone tissue engineering construct, pore size must be within a particular range as pores have to be large enough for cellular in-growth, nutrient and waste exchange [67] yet be small enough to maximize surface area for optimal cell binding to the substrate[68]. In this study, the significant change in porosity is probably the main reason that prevents penetration of cells into the scaffold as demonstrated in Figure 6.

Multiple bands of the control or released DNA shown in the gel represent the various conformations of the plasmid. The predominant band of the control is likely the linear plasmid according to the ladder and the top one may represent nicked/relaxed circular plasmid[69]. The top bands of the released GFP DNA plasmid remained at the same position as the control, which may indicate that the released DNA of nicked/relaxed conformation retained its size and presumably its structural integrity (this part of the released DNA has survived both the electrospinning process and the post-processing conditions of scaffold incubation and sample precipitation). However, the released DNA of linear conformation is behind the linear band of the control, indicating that this part of released plasmid might have been changed and lost its bioactivity, which is consistent with the transfection result using Fugene HD, showing a decrease of transfection efficiency from 50% to 14% using the same amount of GFP plasmid DNA. In addition, the released DNA sticking in the gel loading well indicates either the size of the released DNA is too big (probably complexed with the PLGA or PELA polymers) to migrate through the gel or the released DNA has no negative charge any more.

Cells plated on the GFP containing scaffold did not show very good viability based on their morphology shown in Figure 6, which appear small and round. The size of the cells is even smaller than the diameter of the fibers. Further quantitative proliferation assays are needed to confirm the cell viability plated on the scaffold. Probably the shrinkage of the scaffold also played a role in this low viability effect. As the scaffold shrunk, the cells adhered on it may be “squeezed” and thus damaged leading to loss of viability.

The transfection efficiency of the GFP DNA scaffold is higher than that of the no DNA control scaffold (group 1), no GFP DNA scaffold with Fugene HD (group 2) and no GFP DNA scaffold with additional GFP (group 3). This illustrates that first, the GFP DNA scaffold has the ability of delivering the GFP plasmid into cells plated on it; second, the gene delivery efficiency of GFP scaffold is higher than naked DNA delivery; and the GFP plasmid is bioactive, that is capable of being transcribed. However, the transfection efficiency of the GFP scaffold was still at a very low level (~0.37%). This efficiency is slightly lower than GFP scaffold with Fugene HD reagent supplemented in cell culture medium (group 6, 0.57%), and much lower than just using scaffold (with or without DNA) with supplemental lipid/DNA complexes in cell culture medium (group 4 or 7, 2.08% and 2.85%, respectively). In summary, these results indicate that the DNA containing electrospun scaffold has a very limited transfection capability, and gene delivery using lipid/DNA complexes is much more efficient (7-9 fold). Overall, the transfection efficiency of all of these approaches is very low (lower than 3%), which may be due to the low cell viability resulting from scaffold shrinkage or damage of the plasmid DNA.

2.4 Conclusion

A DNA incorporated PLGA/PELA based scaffold has been successfully fabricated. The scaffold has a porous structure with an overall fiber size about a micron. DNA is successfully released from the scaffold and partially retains its size integrity, transfection efficiency and bioactivity. However, cells plated on the scaffold did not migrate into the scaffold and probably did not survive, as a result of scaffold shrinkage.

Based on these results, another type of electrospun scaffold previously fabricated by out laboratory[34] mainly using a different type of polymer, PLLA, which is not known to shrink as PLGA does in an aqueous environment (i.e. culture medium) was employed and further modified for BMP-2 gene delivery and bone formation.

Figure 1. PLGA/PELA scaffold morphology. SEM images showing: a) GFP DNA containing scaffold. b) Scaffold with no DNA.

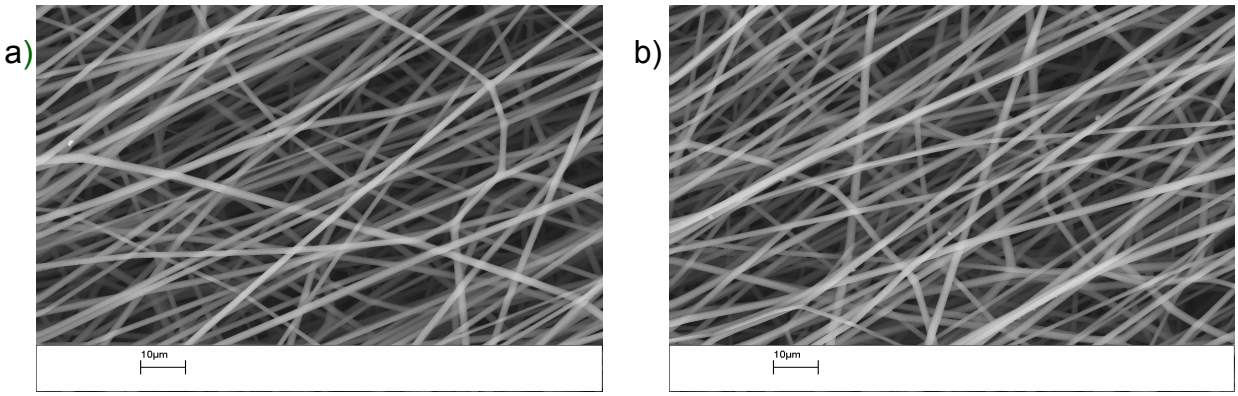

Figure 2. DNA release from electrospun scaffolds. Six pieces (1.5cm×1 cm each) of GFP DNA scaffold were incubated in TE buffer at 37ºC, and PicoGreen quantification were performed in triplicate for each sample. Values are mean±S.D., n=6 scaffolds.

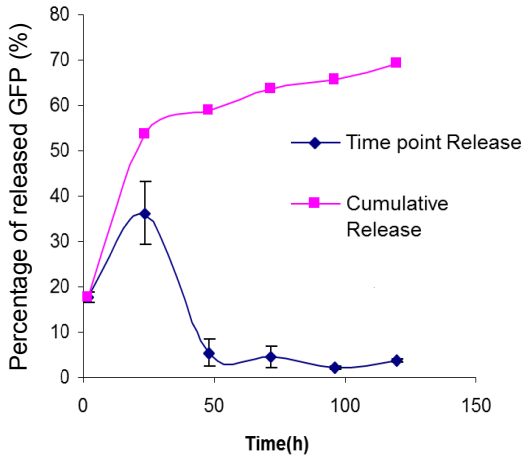

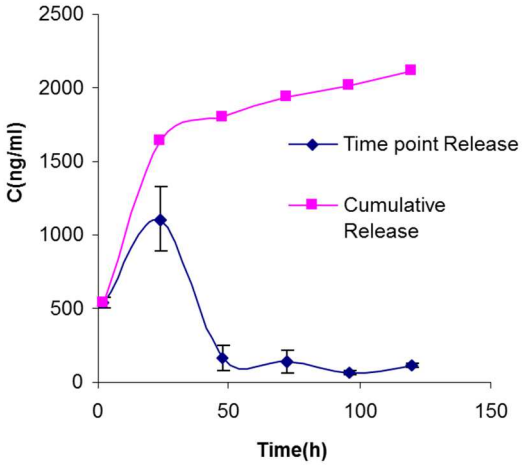

Figure 3. Integrity of released plasmid DNA. Lane 1: molecular weight marker (1kb); lane 2: unincorporated control plasmid DNA, lane 3, 4, 5 and 6: 2h 1d, 3d, and 5d released DNA.

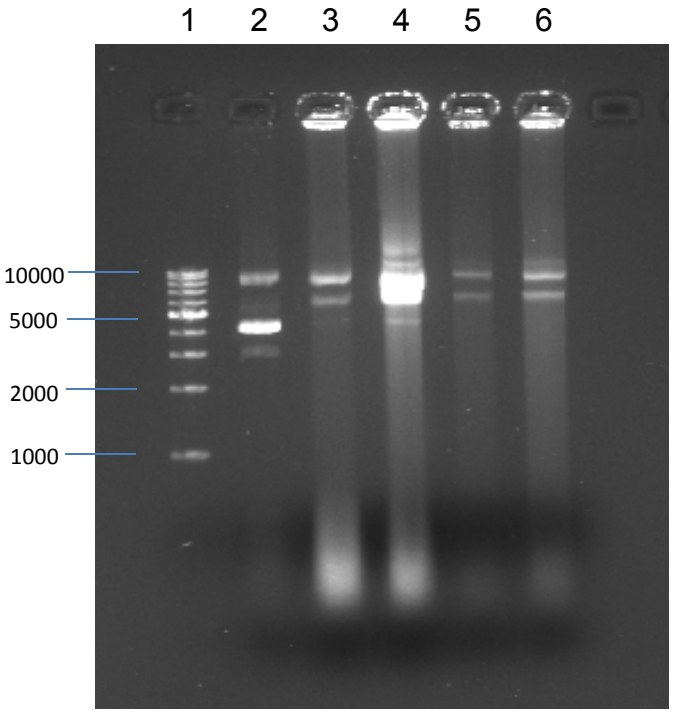

Figure 4. Expression of released GFP transfected by Fugene HD visualized by fluorescence microscopy. Left: MC3T3 cells in 24-well plate transfected by released GFP/Fugene HD complexes (500ng DNA/well). Right: MC3T3 cells in 24-well plate transfected by original GFP/Fugene HD complexes (500ng DNA/well).

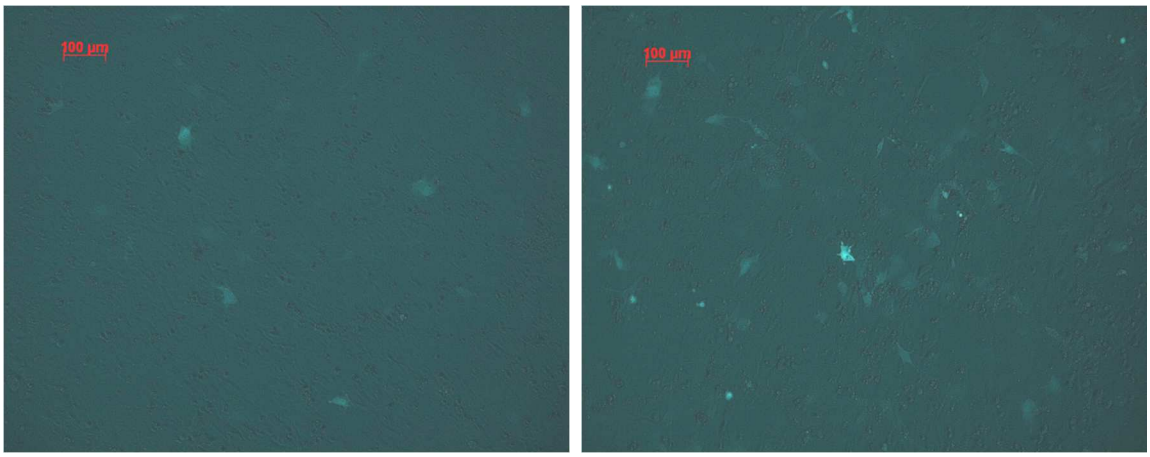

Figure 5. Transfection efficiency of released and unincorporated GFP delivered without any vector (naked plasmid) or complexed with Fugene HD transfection reagent and quantified by FACS. Values are mean±S.D., n=4. 1: naked GFP plasmid released in TE buffer; 2: GFP released in TE buffer complexed with Fugene HD; 3: naked original GFP; 4: Original GFP complexed with Fugene HD complexes; 5: No GFP, cells only. Group 2 and 4 have significant difference with each other and group 1, 3 and 5 ($p<0.001$), respectively. There is no significant difference between group 1,3 and 5 ($p>0.05$).

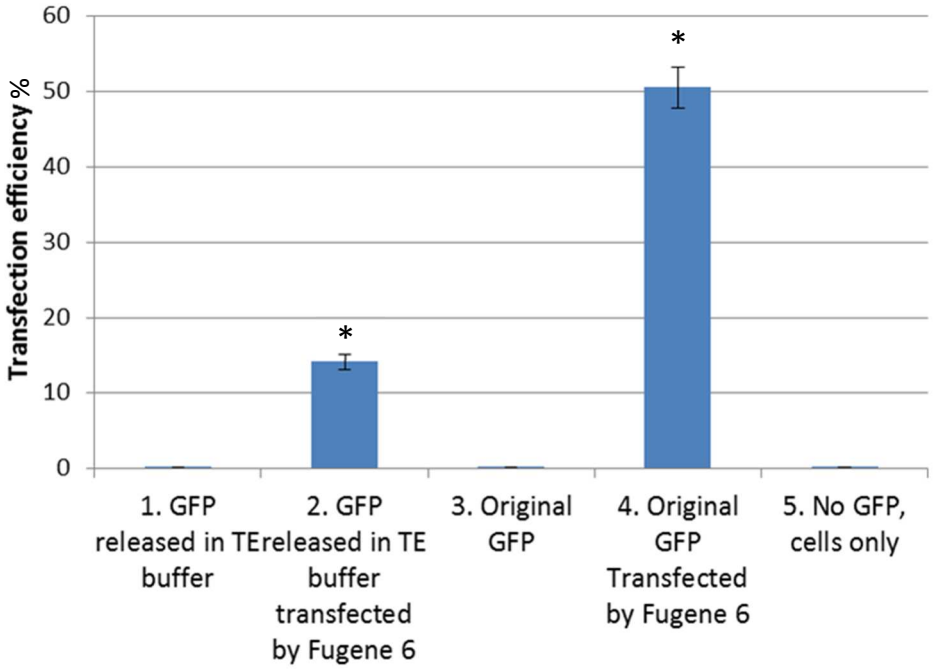

Figure 6. Morphology of MC3T3 cell seeding on the GFP DNA containing PLGA/PELA scaffold for 3 days stained by nuclear fast red reagent.

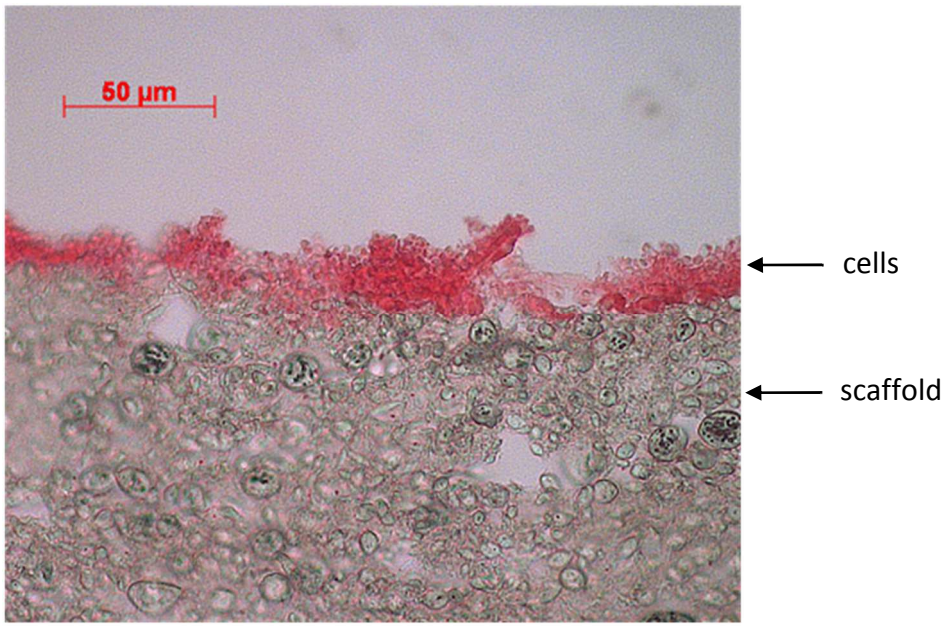

Figure 7. Quantification of GFP scaffold transfection efficiency as determined by FACS. Values are mean±S.D., n=3 . 1: No GFP scaffold only; 2: No GFP scaffold w/ Fugene HD; 3: No GFP scaffold w/ original GFP plasmid ; 4: No GFP scaffold w/ original GFP/Fugene HD complex; 5: GFP scaffold only; 6: GFP scaffold w/ Fugene HD; 7: GFP scaffold w/ Original GFP/Fugene HD complex. Group 4 and 7 have significant difference with group 1, 2, 3, 5 and 6, respectively ($p<0.01$, * labeled), but do not have significant difference between each other ($p>0.05$). There is also no significant difference between any two of Group 1, 2, 3, 5 and 6 ($p>0.05$)

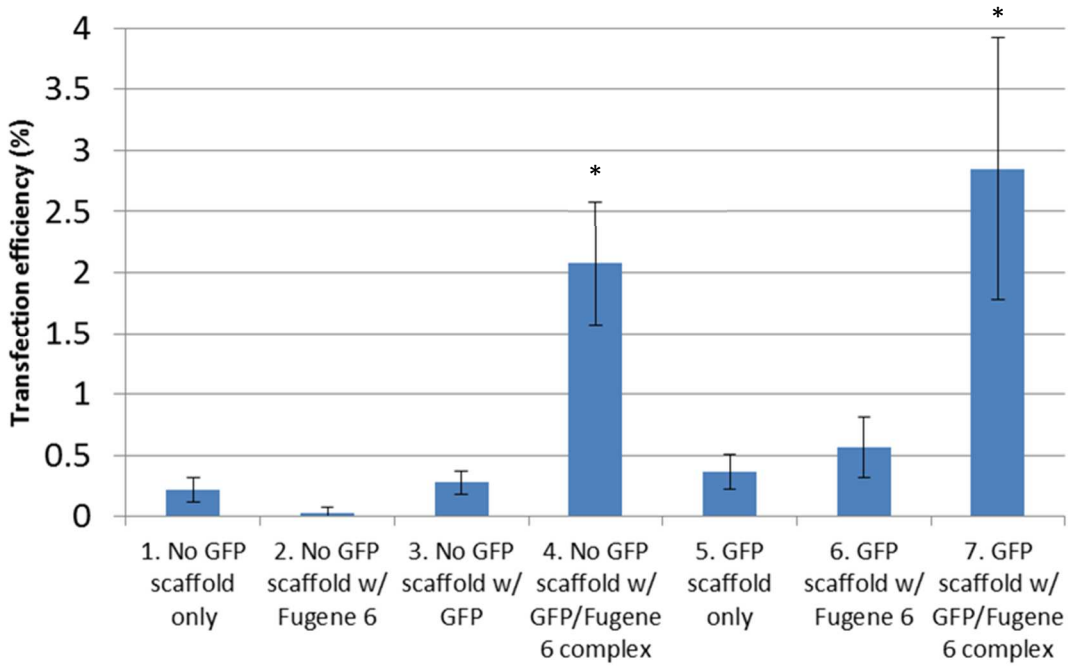

3 Specific aim 2

Evaluating the ability of an electrospun collagen/PLLA scaffold with surface adsorbed BMP-2 DNA transfection complexes to deliver BMP-2 DNA and stimulate preosteoblast differentiation *in vitro*.

The original description of the fabrication of electrospun collagen/PLLA scaffold and its investigation on cell behavior was previously reported by our laboratory[34]. In this specific aim, the previously fabricated scaffold was cut into sections and soaked in transfection complex solutions to absorb the complexes. Then cells were plated onto the transfection complex containing scaffold to test its transfection efficacy *in vitro*.

3.1 Materials and Methods

3.1.1 Transfection of Hela cells using collagen/PLLA scaffold with surface immobilized β-gal plasmid DNA/lipid complexes

3.1.1.1 β-gal plasmid DNA/lipid complex synthesis and immobilization

DNA/lipid complexes were formed by mixing plasmid with TrueFect-Lipo™ Transfection reagent (United Biosystems, Rockville, MD). To make 125μl of lipid/β-gal DNA complexes, 1μg β-gal plasmid DNA was dissolved in 121μl of water and then 4μl of the reagent was added into the DNA solution. The mixture was vortexed immediately after the addition of the reagent for 1 second. Complexes were subsequently incubated at RT for 15 min before immobilization (substrate-mediated) or addition to culture media (bolus). Scaffold was punched into round discs using a puncher (diameter of 7mm) and

sterilized by dipping into absolute alcohol for 15 minutes. After being removed out of the alcohol, the scaffold sections were air dried over night. Then each scaffold disc was submerged into and entirely covered by 50µl of lipid/DNA complex suspension in an Eppendorf tube for 5 hours. Subsequently the scaffold discs were transferred to a 96-well tissue culture plate with or without air drying before proceeding to the next transfection step.

3.1.1.2 Transfection

To initially test our scaffold, we used a common cell line (Hela). These cells were cultured in DMEM with 10% (v/v) FBS, 1% (v/v) penicillin streptomycin at 5% CO_2, 37°C, and 95% humidity. For transfection, cells were seeded on the dried or undried scaffold discs at a density of 3×10^4cells/well for 48 h. For positive control, scaffold discs without any complex immobilization were placed onto the 96-well plate. Then, the same amount of cells suspended in 100µl medium were mixed with 50µl of lipid/DNA complex suspension and plated onto each scaffold disc. For negative control, 3×10^4 cells were seeded onto each scaffold disc placed on the bottom of the 96-well plate. All experimental conditions were performed in triplicate.

48 hours after transfection, the cells were fixed on the scaffolds with 10% formalin. The expression of β-galactosidase was visualized by staining with X-gal solution for 24 hours. Upon removing of the X-gal solution the cells were counter stained with nuclear fast red reagent for 5 min and washed twice with distilled water. The scaffold discs were then dried and photographed using a Zeiss microscope (Axiovert 200 equiped with a digital camera).

The obtained images were processed using Matlab to quantify the transfection efficiency. First, the images were converted from RGB to HSV colorspace. Then, typical areas of low and high saturation of red and blue color were chosen to define the H and S threshold values of each color. Using the color threshold, the total pixels of red color and blue color was calculated and the pixel ratio of blue color and the sum of red and blue color was calculated as the transfection efficiency.

Transfection efficiency = total pixels of blue color / (total pixels of red color+total pixels of blue color)

3.1.2 Induction of preosteoblast differentiation by transfection of MC3T3 cells using collagen/PLLA scaffold with surface immobilized BMP2 plasmid DNA transfection complexes

3.1.2.1 Cell culture

Following the preliminary experiments using Hela cells, preosteoblastic MC3T3 cells were then used as our model for osteogenic differentiation and were cultured in αMEM (α modified Eagle medium) supplemented with 10% FBS and 1% Penicillin/Streptomycin at 37ºC with 5% CO_2.

3.1.2.2 Preparation of transfection complexes

BMP2 transfection complexes were prepared using Xfect Transfection Reagent (Clontech, CA) following manufacture's protocol. To make 80μl of BMP2 transfection complexes, 2μg BMP2 plasmid was diluted by the Xfect Reaction Buffer to a total

volume of 40µl, and 0.6µl Xfect Polymer was also diluted in the Xfect Reaction Buffer to 40µl. The polymer solution was added to the DNA solution and the mixture was vortexed for 10 seconds and then incubated at RT for 10 min.

3.1.2.3 Transfection

The collagen/PLLA scaffolds were cut into discs using a hole puncher (diameter of 14mm), sterilized by submerging into 70% EtOH for 15 min, and then washed three times with PBS. The sterilized scaffold discs were placed into 24-well plates one piece per well and 80µl of BMP2 transfection complexes (equals to 2µg DNA) (experimental: represented by "BMP2 scaffold" group)or PBS (negative control: represented by "scaffold only" group) were added into each well for an overnight incubation at RT. Subsequently, the transfection complexes or PBS were removed and 2×10^4 MC3T3 cells were seeded onto each scaffold section. After the transfection, cells were incubated in mineralization medium (500µl/well) composed of αMEM supplemented with 10% FBS, 1% Penicillin/Streptomycin, ascorbic acid (100 µg/ml) and β-glycerophosphate (100 mM) [34]. The medium was changed every 2-3 days.

3.1.2.4 Quantitative real-time PCR

After 3 and 7 days of transfection, cells were subjected to total RNA extraction using an RNAeasy Mini Kit (QIAGEN, Valencia, USA). Cells plated onto collagen/PLLA scaffold discs without transfection complex immobilization served as a control. Quantitative real-time PCR (qRT-PCR) was carried out with QuantiTect SYBR Green RT-PCR Kit (QIAGEN, Valencia, USA) following the standard protocol for the

LightCycler system (Roche, Indianapolis, USA). BMP2, RUNX2 and OSX were assayed as target osteoblast differentiation marker genes. GAPDH served as a housekeeping gene. The copy number ratio of the target gene relative to the reference gene was obtained first for control and experimental group and then the ratio of the control "scaffold only" group was normalized to 1 for comparing the experimental "BMP2 scaffold" group. This experiment was performed in triplicate.

3.1.2.5 ELISA

On day 3, day 7 and day 14 of transfection, cell culture medium was collected from each well and stored at -20ºC until all the time points were collected and assayed for quantitative determination of BMP-2 protein levels using a Quantikine BMP2 immunoassay kit (R&D systems, MN) following manufacture's protocol. This experiment was performed in quadruple.

3.1.2.6 Alizarin Red staining.

Alizarin Red S staining was performed to determine the amount of mineralized matrix produced by the cells[70]. On day 14, day 21 and day 28 of transfection, cells were fixed in 4% paraformaldhyde for 15 min and stained in 40mM Alizarin Red-s reagent at pH 4.2 for 10 min at RT. After 5 times of wash by water, the cells were photographed and then destained for 15 min with 500 µl of 10% (w/v) cetylpyridinium chloride(CPC) dissolved in 10mM sodium phosphate (pH 7.0). Subsequently, the extracted stain was transferred to a 96 well plate and measured at 562 nm in a plate reader[71]. This experiment was performed in quadruple.

3.1.2.7 statistics

One-tailed Welch's t-test which do not assume equal variances was used to determine significant difference between control and BMP2 scaffold group for qRT-PCR, ELISA and Alizarin Red staining at each time point.

3.2 Results

3.2.1 Transfection of Hela cells using collagen/PLLA scaffold with immobilized β-gal plasmid DNA/lipid complexes

Cells seeded on the scaffold discs with or without adsorbed lipid/DNA complexes after 48 hrs grew along the fibers and had the same spindle-shaped morphology (Fig. 1), which is consistent with our precious study[34]. Results from the transfection experiments show that the scaffold with undried lipid/DNA complex immobilization retained the transfection ability of the complexes and had a transfection efficiency of 37±7% (Fig. 1b, e & g). This efficiency is lower than the control (Fig 1c & f), which had cells seeded on the collagen/PLLA scaffold transfected by lipoplexes supplemented in the medium, with 90±5% cells transfected (Fig. 1g). The experimental group with dried immobilized lipid/DNA complexes did not have any positive β-gal expression (Fig. 1d), as was the case with the negative control (Fig. 1a), i.e., the transfection efficiency of both of the two groups is 0 (Fig. 1g).

3.2.2 Induction of preosteoblast differentiation by transfection of MC3T3 cells using collagen/PLLA scaffold with immobilized BMP2 plasmid transfection complexes

3.2.2.1 Real time PCR analysis of mRNA level of gene expression

To confirm the effective transfection of MC3T3 cells by the BMP2 transfection complex immobilized scaffold (BMP2 scaffold), and the osteogenic differentiation induced by the expressed BMP2 protein, expression of BMP2 and the marker genes of osteogenesis including OSX and RUNX2 was evaluated by real-time PCR (figure 2). Significant (more than 40 fold and 10 fold) increase of BMP2 mRNA level was observed on day 3 and day 7 of transfection, showing that the MC3T3 cells were successfully transfected by the BMP2 scaffold, which means that the adsorbed BMP2 plasmid transfection complexes retained their bioactivity after immobilization. A 1.5 fold increase of mOSX mRNA level was observed on day 3 of transfection, which is significantly different from the control. About 3 fold increase of OSX and RUNX2 mRNA level (3.20 and 2.97, respectively) was observed on day 7 of transfection, however, the increase is not statistically significant in comparison with control, which means that the delivered BMP2 gene may not induce osteogenic differentiation, as measured by these molecular marker genes (Figure 2).

3.2.2.2 ELISA

To confirm that the protein product of the delivered and expressed BMP2 gene was secreted and present in the cell culture medium, ELISA was performed (Figure 3). In contrast to the real-time PCR results, no significant BMP2 protein expression was detected. A number of possibilities can account for these results and they are: (1) no BMP2 protein secreted into the cell culture medium; (2) the secreted BMP2

concentration was very low to be detected via ELISA; and (3) the secreted BMP2 protein was rapidly degraded.

3.2.2.3 Alizarin red staining

Similar to the ELISA results, the Alizarin red staining for mineralization of extra cellular matrix did not show significant difference between the experimental group and the control group at all time points tested (Figure 4).

3.3 Discussion

3.3.1 Transfection of Hela cells using lipid/β-gal complex loaded collagen/PLLA scaffold

The undried lipid/DNA complexes were adsorbed onto the collagen/PLLA scaffold and showed robust transfection efficiency, in contrast to the dried immobilized lipid/DNA complexes whose transfection efficiency was nonexistent. One reason may be that the drying process destroyed the structure of the lipid/DNA complexes and thus affected the transfection capability of the complexes.

The transfection efficiency of the undried GFP scaffold was lower than that of the positive control. This phenomenon may have resulted from the loss of the complexes which were not adsorbed onto the scaffold discs in comparison with those added in the positive control.

The mechanism of the adsorption process is not clear. The adsorption between the scaffold and the lipid/DNA complexes may be due to some surface interactions

including electrostatic interaction, hydrophobic interaction, hydrogen bonding and Van der Waals force[72]. It is known that the lipid/DNA complexes are positively charged. We observed that the scaffold had some electrostatic charges on its surface after the electrospinning process. So it is highly possible that the adsorption is mainly driven by electrostatic force. Another possibility is that the porous structure of the scaffold held some of the complex suspension inside the pores like a sponge and the complexes were released into the cell culture medium again during the transfection. Further investigation is needed to verify the exact immobilization mechanism but it is beyond the main scope of this thesis.

3.3.2 Transfection of MC3T2 cells using BMP2 transfection complex loaded collagen/PLLA scaffold for induction of preosteoblast differentiation

In this study of induction of osteogenic differentiation by BMP2 transfection complex adsorbed electrospun collagen/PLLA scafffold, conflicting results were obtained. On one hand, MC3T3 cells were successfully transfected by the BMP2 scaffold with significant upregulation of BMP2 at the mRNA level, showing the transfection complexes were successfully immobilized on the surface of the collagen/PLLA scaffold and retained their bioactivity. On the other hand, the BMP2 protein level was not detected, and the mineralization of extracellular matrix was not enhanced by the cell transfection using the BMP2 scaffold. This conflicting observation may result from the cytotoxicity of the transfection reagent. During our experiments we observed that the transfection reagent was very toxic to the MC3T3 cells and following transfection. Specifically, by day 3 after transfection, few cells were left on the scaffold

as visualized by nuclear fast red staining (data not shown). Hence, we speculate that even though the cells were successfully transfected, a large number of cells died and the BMP2 protein produced by the cells that were still alive was diluted by the cell culture medium and thus it was not detectable by ELISA. Although the mRNA level of OSX and RUNX2 were upregulated, they were not significant enough to compensate for the effect of cell loss on mineralization. Thus there was no enhancement of mineralization detected at the later time points (days 14-28). Another speculation is that, although there was BMP2 protein expressed by the transfected cells, the protein was quickly degraded by the proteases in the cell culture medium. It was previously reported that BMP2 has a very short half-life of 7-16 min *in vivo*[73]. If the same is true *in vitro*, then the protein level of BMP2 may not be detectable on the time points that we tested (day 3, 7 and 14) after transfection.

Alizarin Red S is widely used for calcium mineral histochemistry because of its selectivity to calcium salts [74]. However, Alizarin Red S staining itself is not sufficient enough to prove the calcium mineral is specifically hydroxyapatite and has the correct mineral phase, similar to the native bone mineral[75]. Further analysis using energy-dispersive X-ray spectrometry (EDS), X-ray diffraction (XRD), FTIR etc. is needed to determine elemental composition, crystallinity, and other properties of the formed mineral[75]. Because there is no augmentation of mineralization found between the control and transfected BMP2 plasmid group, further analyses were not performed.

Although the protein level of BMP2 and augmentation of mineralization were not detected *in vitro* most likely due to the cytotoxicity of the Xfect transfection reagent, it

may not be as potent *in vivo* because the *in vivo* environment is different. Moreover, the Xfect transfection reagent creates biodegradable nanoparticles with plasmid DNA according to the manufacturer. Compared to other commercially available transfection reagents including the TrueFect-Lipo^{TM} Transfection reagent, which produces lipoplexes with plasmid DNA, the product is easy to use and compatible to serum in the tissue culture medium whereas lipid based transfection reagents are not compatible to serum. Taken the above two reasons together, we choose this Xfect transfection reagent for our *in vivo* study.

3.4 Conclusion

The electrospun collagen/PLLA scaffold with surface adsorbed lipid/DNA complexes is able to transfect Hela cells seeded onto the scaffold efficiently. In addition, the electrospun collagen/PLLA scaffold with surface adsorbed BMP2 nanoparticle transfection complexes is able to successfully transfect MC3T3 cells seeded onto the scaffold and BMP2 mRNA was produced. However, BMP2 protein secretion and enhancement of osteoblast differentiation was not detected probably due to the cytotoxicity of the transfection reagent used.

Figure 1. *In vitro* transfection using collagen/PLLA scaffold with surface adsorbed DNA/lipid complexes and quantified transfection efficiency. a) Negative control, cells plated on collagen/PLLA scaffold only, without any adsorbed DNA/lipid complexes. b) Cells transfected by seeding on collagen/PLLA scaffold with surface adsorbed β-gal plasmid/lipid complexes. c) Cells plated on collagen/PLLA scaffold transfected by β-gal plasmid/lipid complexes supplemented in cell culture medium. d) Cells transfected by seeding on collagen/PLLA scaffold with dried surface adsorbed β-gal plasmid/lipid complexes. e) Higher magnification of cells from condition b). f) Higher magnification of cells from condition c). g) Quantified transfection efficiency of condition a), b), c) and d). Scale bar: 50μm.

a)

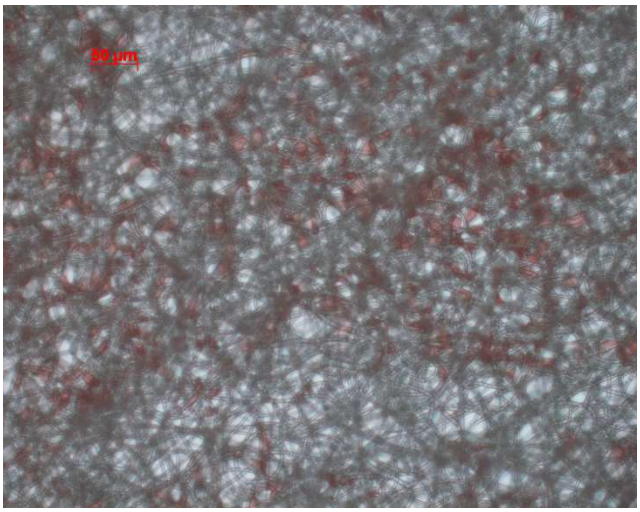

b)

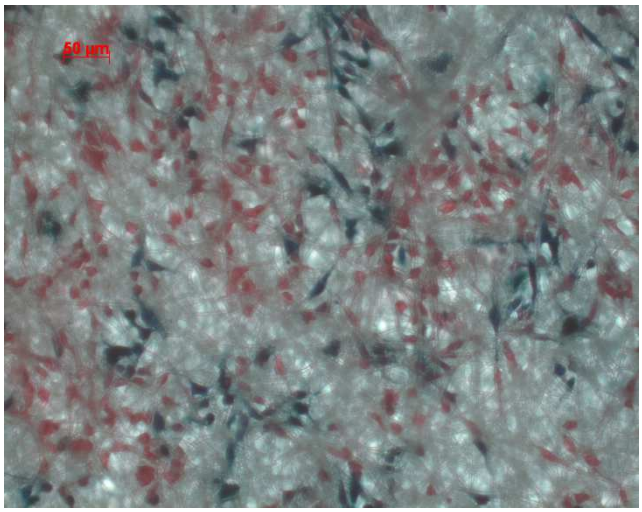

c)

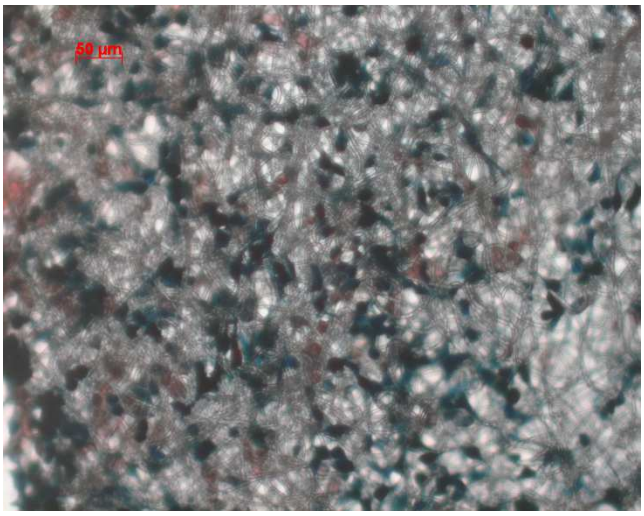

d)

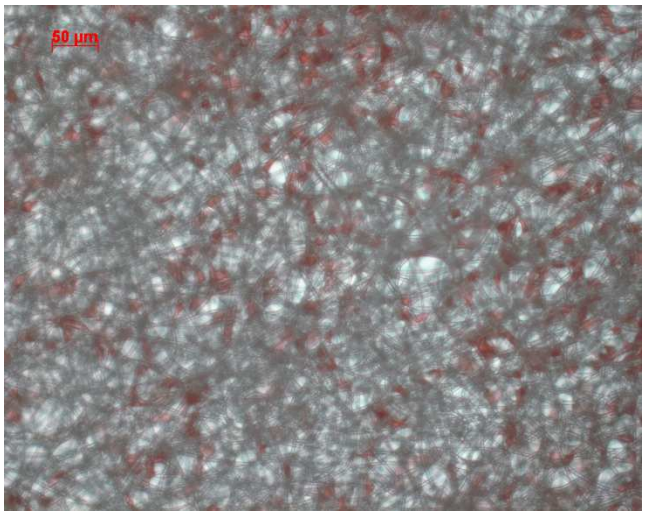

e)

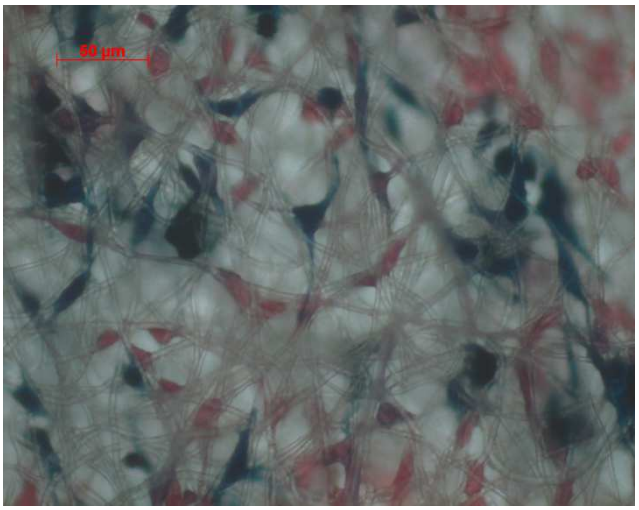
50 µm

f)

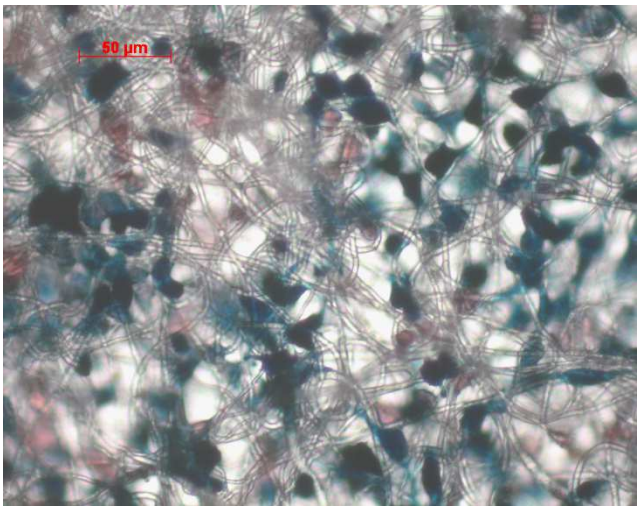
50 µm

g)

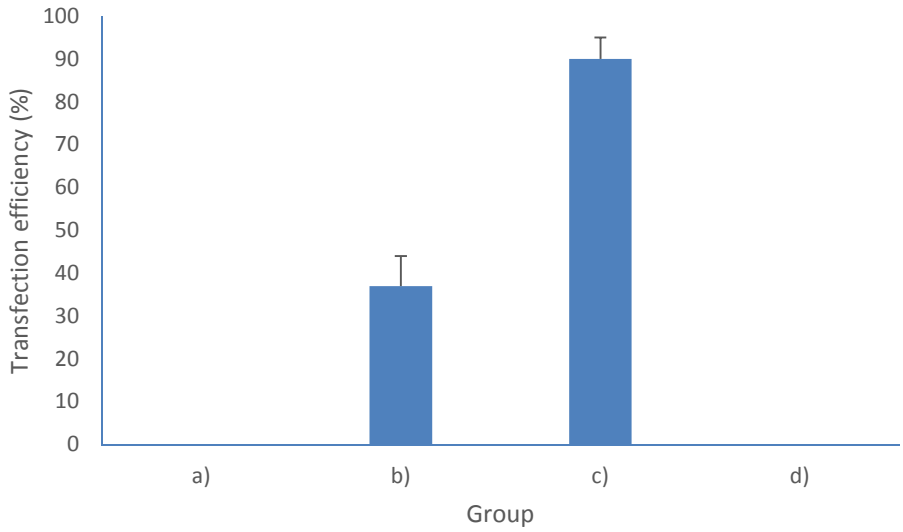
Transfection efficiency (%)
100
90
80
70
60
50
40
30
20
10
0
a)
b)
c)
d)
Group

Figure 2. mRNA level of BMP2, RUNX2 and OSX after transfection using control scaffold at day 3, BMP2 scaffold at day 3, control scaffold at day 7, and BMP2 scaffold at day 7. The copy number ratio of the target gene (BMP2, RUNX2 and OSX) relative to the reference gene (GAPDH) was obtained first for control and experimental group and then the ratio of the control "scaffold only" group was normalized to 1 for comparing the experimental "BMP2 scaffold" group. * represents $p<0.05$ comparing to control.

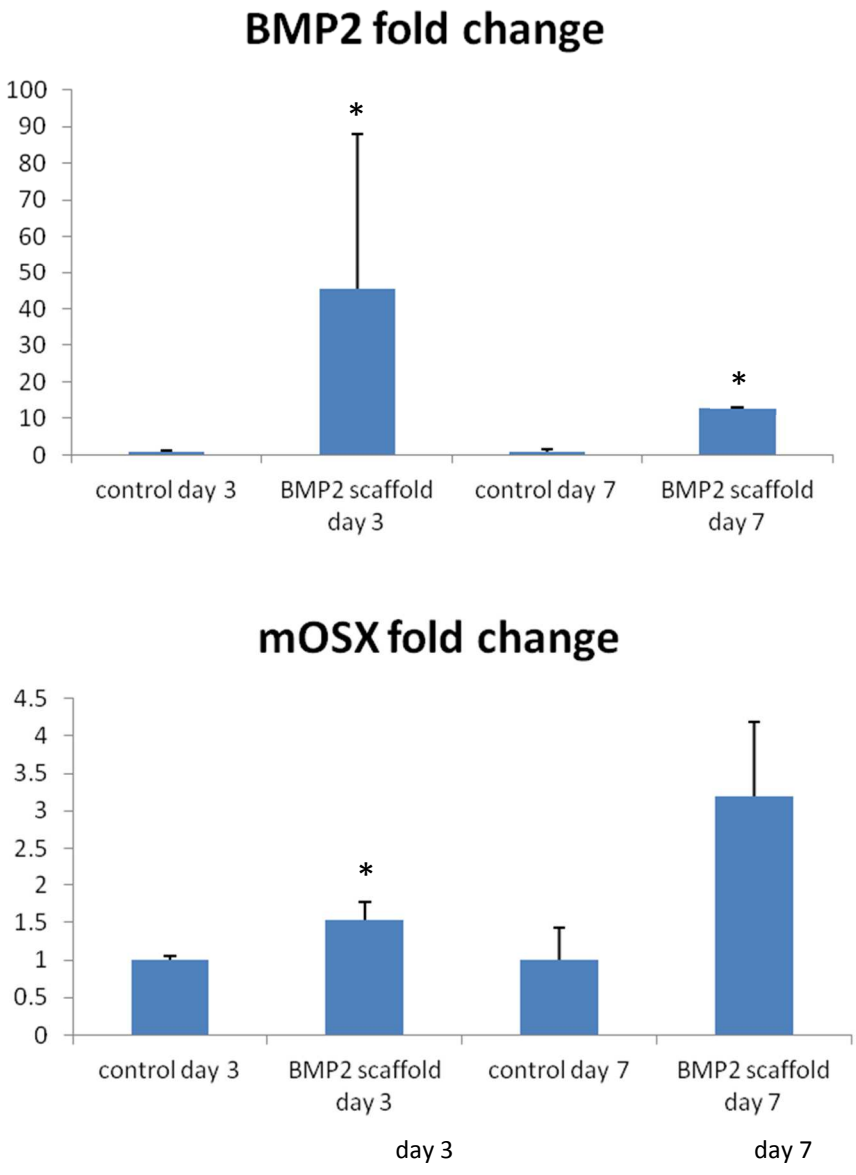

Figure 3. Quantitative determination of BMP2 protein concentration in cell culture medium at different time points (day 3, 7, and 14) post-transfection using ELISA. Control: collagen/PLLA scaffolds with MC3T3 cells seeded on them. BMP2: BMP2 containing collagen/PLLA scaffolds with MC3T3 cells seeded on them.

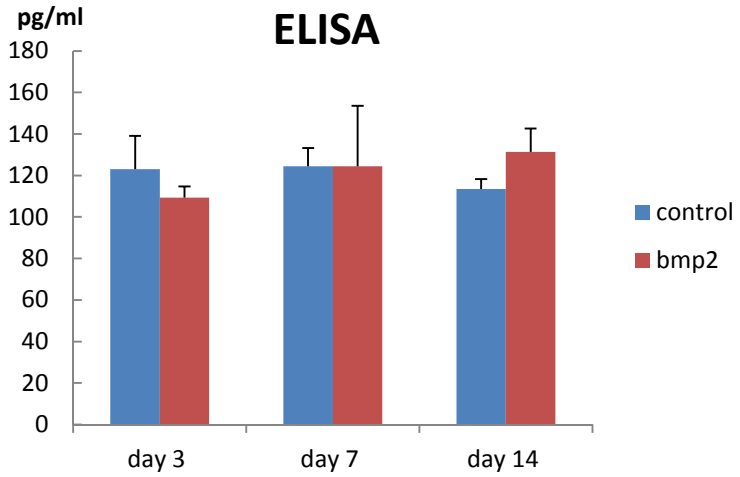

Figure 4. A) Alizarin red staining of transfected cells seeded on control scaffold and BMP2 containing scaffold on post-transfection day 14, 21 and 28. Cells in each column are in the same condition. B) Alizarin red staining elute using 10% CPC and detected by a spectrometer at 562nm.

A

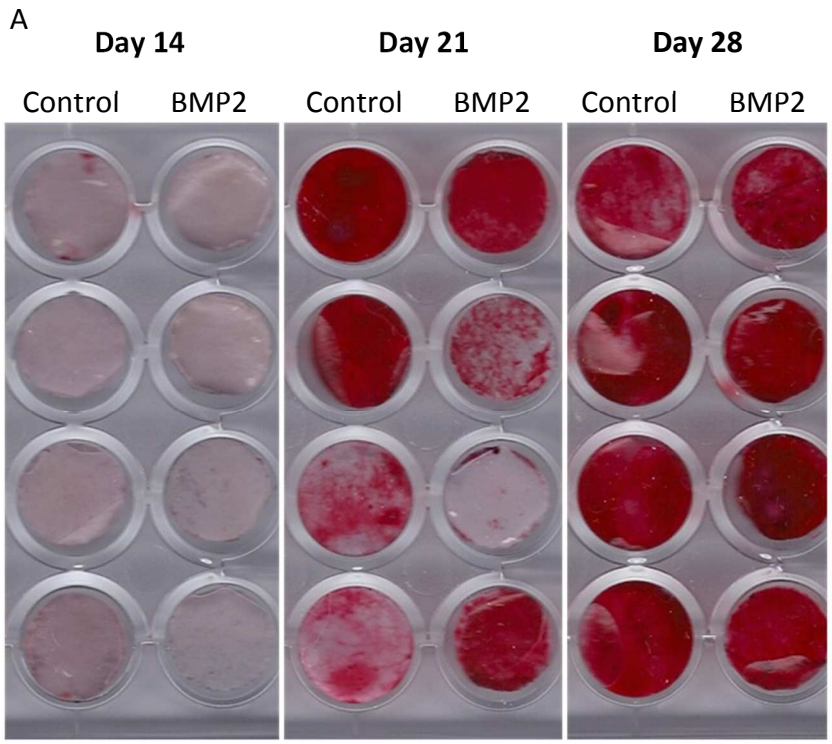

B

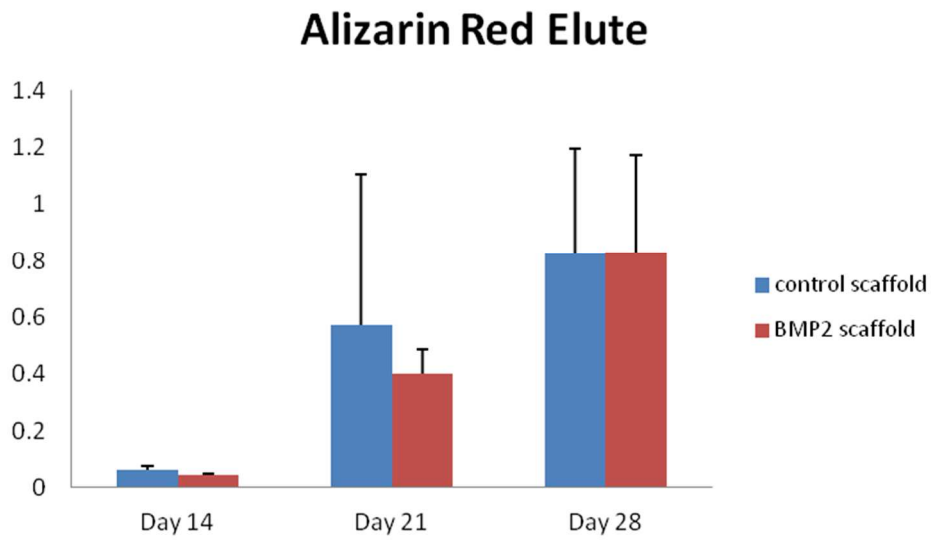

4 Specific aim 3

Assessing the ability of the electrospun collagen/PLLA scaffold with surface adsorbed transfection complexes to deliver BMP-2 plasmid and induce ectopic bone formation *in vivo*.

In this specific aim, the collagen/PLLA scaffold with surface adsorbed BMP2 transfection complexes was implanted *in vivo* using a mouse thigh muscle pouch model for induction of ectopic bone formation. β-gal was used as a reporter gene for evaluating the transfection. X-gal staining, qRT-PCR, IHC, microCT and Alizarin red staining was performed for analyzing the gene delivery and bone formation process.

4.1 Materials and methods

4.1.1 Experimental and control groups

The groups, animal numbers for each analysis and time points are summarized in Table 1. Each animal represents two samples because the surgery was done bilaterally as described below. The five groups are: 1) "scaffold only", 2) "scaffold+β-gal complexes", 3) "scaffold+BMP2 complexes", 4) "BMP2 complexes injection", and 5) "scaffold+BMP2 protein". On day 3 and 7, X-gal staining was performed on group 1&2, qRT-PCR and IHC were performed on group 1, 3 and 5 samples. On day 14 and 28, microCT and histology analysis were performed on all five group samples.

4.1.2 Animals and surgery

Male (28-31 day) Swiss Webster mice (Charles River, USA) were used to test the *in vivo* gene delivery efficacy of the collagen/PLLA scaffold with surface adsorbed transfection complexes [76, 77]. Scaffolds were cut into circular discs using a hole puncher with diameter of 7mm, submerged into 70% EtOH for 15 minutes, and then washed three times using PBS. One day before surgery, the DNA (β-gal or rhBMP-2) transfection complexes were prepared and immobilized onto the scaffold discs as described in section 3.1.2.2 and 3.1.2.3. To prepare the positive control discs, 1μg rhBMP2 protein (R&D systems) was dissolved in 10μl water and immobilized onto each scaffold disc. On the day of surgery, the mice were anesthetized by an intraperitoneal injection of ketamine/xylazine (100mg/10mg per kg). The fur on the target area of each leg was shaved with a clipper. A 2–3 mm skin incision overlying the gracilis (figure 1) was made using scissors[78]. Then a muscle pouch was generated on the musculature along the muscle fibers and a collagen/PLLA scaffold disc with or without surface adsorbed transfection complexes was inserted into the muscle pouch. The skin incisions were closed by suturing[79]. For the BMP2 transfection complex injection group, 50μl of transfection complex solution was injected directly in to the target area of the surgery. At post-surgery day 3, 7, 14, and 28, the mice were sacrificed, and the scaffolds and surrounding tissue or the tissue around the injection site were harvested for analysis (Table 1).

4.1.3 Embedding and sectioning of harvested tissue

The specimens were fixed in 4% paraformaldehyde at 4 ºC for 24 hrs. After rinsing at RT in PBS with 5% sucrose, the specimens were cryoprotected through the

following steps: 1) infiltrated by increasing concentrations of sucrose by mixing 5% and 20% sucrose in PBS in ratios of 2:1, 1:1, 1:2, each for 30 min at RT, 2) then with 20% sucrose in PBS at 4 ºC overnight, 3) infiltrated in a mixture of 2 parts 20% sucrose to 1 part Tissue-Tek O.C.T. (Sakura Finetek Co. Ltd., Tokyo, Japan) embedding medium for 30 min at RT. All of the above fixation, rinses and infiltrations were done with gentle rotation [80].

After fixation and cryopreservation, the specimens were embedded in infiltration mixture (2:1 20% sucrose : O.C.T.) and frozen in liquid nitrogen cooled isopentane [80]. The samples were then cut into 20 μm sections on a cryostat and placed on glass slides.

4.1.4 X-gal staining

Tissue/scaffold sections were stained with X-gal reagent containing 1 mg/ml X-gal, 2 mM $MgCl_2$, 5 mM $K_4Fe(CN)_6$, 5 mM $K_3Fe(CN)_6$ at 37 ºC overnight, and then mounted in AQUA-POLY/MOUNT (Polysciences, Inc. PA USA) mounting medium after washing and observed under a Zeiss Axiovert 200M microscope. Minimum 6 sections were analyzed for each sample.

4.1.5 Quantitative real time-PCR (qRT-PCR)

mRNA expression of the transfected BMP2 and its downstream genes, RUNX2, OSX, OSC, COL1A1, were detected using qRT-PCR. Total RNA samples were extracted from the harvested day 3 and day 7 specimens of control "scaffold only" and experimental "scaffold+BMP2 complex" groups using an RNAeasy Mini Kit (QIAGEN,

Valencia, USA). qRT-PCR was carried out with QuantiTect SYBR Green RT-PCR Kit (QIAGEN, Valencia, USA) following the standard protocol for the LightCycler system (Roche, Indianapolis, USA). GAPDH was chosen as a housekeeping gene. The primers used for each gene are shown in Table 2. The copy number ratio of the target gene relative to the reference gene was obtained first for each control and experimental group and then the ratio of the control group was normalized to 1 for comparing the experimental group. The PCR reaction was run three times for each sample.

4.1.6 Immunohistochemical analysis of rhBMP2 protein expression

To investigate if the BMP2 protein was successfully expressed by the *in vivo* transfection using the transfection complex loaded collagen/PLLA scaffold, the scaffolds with surrounding muscles were harvested for immunohistochemical analysis on day 3 and day 7 after implantation/injections. The "scaffold only" group served as a negative control. After embedding and sectioning of the harvested tissue as described previously, the sections were permeabilized with 0.2% Triton X 100 in PBS for 10 min, blocked with 3% horse serum in PBS for 30 min, and then incubated with goat rhBMP-2 antibody (R&D systems) (1:500 dilution) at 4 ºC overnight in blocking solution. Subsequently, after washing, the sections were incubated with a peroxidase labeled rabbit anti-goat secondary antibody (1:1000 dilution), and then visualized using a AEC substrate kit (Vector Laboratories, Burlingame, CA, USA) according to the manufacturer's protocol.

4.1.7 Micro-computed tomography (microCT) analysis of bone formation

MicroCT analysis was conducted on samples harvested after 14 and 28 days of scaffold implantation and analyzed by micro-computed tomography. Following harvesting, the tissue/scaffold specimens were fixed in 4% paraformaldehyde at 4 ºC for 24 hrs. Then, they were transfered into a custom-made, 8-sector partitioned chamber filled with 70% ethanol. The chamber was loaded in the micro-CT apparatus for scanning.

4.1.8 Alizarin Red staining

Alizarin red staining was performed on the day 14 and day 28 samples following surgery and scaffold implantation. After the microCT analysis, these samples were washed by PBS, and cyropreserved and embedded as described in section 4.1.3. Subsequently, the sections were stained with 40mM Alizarin Red solution for 10 minutes at room temperature[71], washed by ddH_2O, mounted using AQUA-POLY/MOUNT (Polysciences, Inc. PA USA) mounting medium and observed under a Zeiss Axiovert 200M microscope Minimum 6 sections of each sample were analyzed.

4.1.9 Statistics

One tailed student's t-test was used to determine significant difference between control and BMP2 scaffold group for qRT-PCR at each time point. One way ANOVA was performed on microCT data on both time points.

4.2 Results

4.2.1 X-gal staining

To easily identify transgene expression after in vivo implantation of the transfection complexes loaded scaffolds, the β-gal gene was used as a reporter gene. Three days and seven days after the implantation, the expression of the β-gal gene was visualized by X-gal staining for β-galactosidase activity. The results of this X-gal staining analysis are summarized in Table 3. In the experimental group "scaffold+β-gal complexes", all of the 4 samples at day 3 and both of the 2 samples at day 7 displayed blue staining. However, 2 out of 4 samples and 3 out of 4 samples of the control group "scaffold only" also had similar blue staining on day 3 and day 7, respectively. Typical pictures of each group at each time point are shown in Figure 2. The blue staining of both the "scaffold only" group and the "scaffold+β-gal complexes" group located surrounding the scaffold. Because some of the control group showed very strong background staining of x-gal on both day 3 (Figure2 A, B) and day 7(Figure 2 E, F), the staining procedure needs further optimization to eliminate the background color.

4.2.2 Real time-PCR

The mRNA level of the rhBMP2 gene after in vivo transfection was detected using real time-PCR. The mRNA level of the mouse RUNX2, OSX, OSC and COL1A1, which are downstream genes of BMP2 and server as markers for osteogenesis, were also determined. RNA isolated from the "scaffold only" group served as a negative control. The result of this analysis is shown in Figure 3. The mRNA level of rhBMP2 in "scaffold+BMP2 complex" group was 5 and 10 times higher than the control on day 3 and day 7, respectively, indicating the rhBMP2 plasmid that was adsorbed on the surface of the Collagen/PLLA scaffold was successfully transfected and expressed by

cells of the surrounding tissue. However, the mRNA level of mRUNX2 gene and mCOL1A1 gene were not upregulated and showed no statistical difference with control. Mouse OSX and OSC mRNA expression was not detected, indicating that mOSX and mOSC were not expressed in the surrounding tissue of the scaffold (data not shown).

4.2.3 Immunohistochemistry analysis of BMP2 protein expression

In agreement with the highly increased BMP2 mRNA level after *in vivo* gene transfer using the "scaffold+BMP2 complex", strong BMP2 protein expression was also detected on day 7 by immunohistochemistry analysis. Table 4. summarizes the results of this IHC analysis. The typical pictures of each group at each time point are shown in Figure 4. All of the samples of "scaffold only" (A/B), "scaffold+BMP2 complexes" (C/D), "scaffold+BMP2 protein" (E/F) groups did not display any rhBMP2 staining on day 3. In contrast, 4 out of 4 samples of "scaffold+BMP2 complexes" group (I/J) showed positive rhBMP2 staining on day 7, whereas 3 out of 4 samples of "scaffold only" group (G/H) did not . Only 1 out of 4 samples of "scaffold only" group displayed background red color staining on day 7, probably due to nonspecific staining (data not shown). The red staining of BMP2 protein mainly located surrounding the scaffolds as shown in Figure 4 G&H.

4.2.4 microCT

The microCT analysis revealed there was much higher amount of bone formation in positive control group with very big variance on day 28, however, the increase of bone formation is not statistically different from other groups. Other groups also did not

show statistically significant amount of bone formation on day 28 (Figure 5). All of the groups did not demonstrate statistically significant bone formation on day 14 (Figure 5).

4.2.5 Alizarin Red staining

Alizarin red staining demonstrated similar result with the microCT analysis. The positive rate of this staining is summarized in Table 5 and typical images of each group on each time point are shown in Figure 6. On day 14, mineralization was observed in 1 out of 4 specimens of "scaffold only" group and except this, no mineralization was found in other control groups including "scaffold+β-gal complexes" and "BMP2 complex injection" group. On day 28, no mineralization was found in all of the three control groups. Mineralization was identified in 3 out of 4 specimens of the positive control "scaffold+BMP2 protein" group on day 14 and 1 out of 4 specimens on day 28. Significantly large calcium nodules (~200μm) only presented in the positive control group in 1 out of 4 specimens on both day 14 (Figure 6 G, H, I) and day 28 (Figure 6 O, P, Q), respectively. Mineralization was also observed in 1 out of 4 specimens with the experimental "scaffold+BMP2 complexes" group on day 14 and 3 out of 4 speciments on day 28 (Table 5), showing that the electrospun collagen/PLLA scaffold with surface immobilized BMP2 transfection complexes successfully induced bone formation. All of the scaffold sections implanted in skeletal muscles were wrapped by fibrous envelops on both day 14 and day 28 (Figure 6) whereas this fibrous envelope did not appear on day 3 and day 7 (Figure 4). Mineralization/calcium nodules were found on the outer edge of the fibrous tissue.

4.3 Discussion

In 1965 Dr. Urist discovered that demineralized bone matrix implanted into skeletal muscle had a bone morphorgenetic property [81].Through a serious of studies he found that robust cartilage and bone was induced from the interior of the demineralized bone after implantation into skeletal muscles of different kinds of animals [81-84]. The inductive substance was found localized in-between the collagen fibers of the demineralized bone and later on was named BMP[83]. Since then, numerous studies emerged to investigate the bone inductive property of BMPs and among those the animal muscle pouch model became a popular model for *in vivo* ectopic bone formation studies [85-88]. In this study, this animal model was also used to investigate the rhBMP2 gene delivery efficacy of the transfection complex loaded electrospun Collagen/PLLA scaffold.

In this specific aim, rhBMP2 gene was successfully delivered into mouse skeletal muscle using Collagen/PLLA scaffold with surface adsorbed transfection complexes. The delivered rhBMP2 gene was transcribed into mRNA, and translated into rhBMP2 protein by day 7 of implantation. The synthesized rhBMP2 protein mainly distributed around the scaffold. Mineralization was histologically detectable at day 14 and day 28 following implantation of scaffolds. However, statistically significant radiographic evidence of ectopic bone was not observed in any group of animals. Implantation into skeletal muscle of scaffold only and scaffold immobilized with β-galactosidase transfection complexes (both negative control conditions), as well as injection of BMP2 transfection complexes (experimental condition) did not produce mineralization/bone, both histologically and radiographically.

This proof of concept study demonstrated the feasibility of rhBMP2 gene delivery into skeletal muscle using transfection complex loaded Collagen/PLLA electrospun scaffold to produce bioactive rhBMP2 protein, and to induce ectopic bone formation and mineralization. Under the present condition, in terms of induction of mineralization, the gene delivery efficacy of the collagen/PLLA scaffold system is better than the direct transfection complex injection approach, though still not as good as the rhBMP2 protein delivery (the gold standard) procedure using the same scaffold. To produce bone, this electrospun collagen/PLLA scaffold gene delivery system needs improvement/optimization and further evaluation in generally three aspects, i.e. gene delivery efficiency, biocompatibility of the tissue engineering scaffold and the combination strategies of the gene delivery system and the tissue engineering scaffold.

First, the gene delivery efficiency of this scaffold delivery system needs to be improved to produce greater amount and/or more suitable release of rhBMP2 protein for bone induction. As a non-viral gene delivery system, the low delivery efficiency is always a problem of this kind of systems when compared to the viral gene delivery systems [89-92]. To improve the delivery efficiency, the transfection complex composition and concentration, and the immobilization means need to be optimized. This study used the polymer-DNA nanoparticle gene delivery system as a vector. The other common non-viral gene delivery vector is liposome mediated [90, 93, 94], which has been shown to be able to produce comparable transfection efficiency close to viral vectors [90]. Switching the gene delivery system to liposome vectors provides one possibility to improve the gene expression level of rhBMP2. The xfect mESC

transfection reagent used in this study was specifically designed for transfection of mESC *in vitro*. The transfection complex synthesis condition and transfection condition suggested by the manufacturer's protocol was only optimized for the *in vitro* transfection of mESCs. In this study, the cell type for transfection, the *in vivo* transfection environment are both different from the *in vitro* conditions provided by the manufacturer's protocol. Hence the transfection complex preparation conditions and the amount of complexes being added to the scaffold needs further optimization. The immobilization means utilized by this study was simply physical attachment between the complexes and the electrospun scaffold. No chemical bonds were involved in the attachment between the complexes and the scaffold. Covalent bonds can be applied for enhanced attachment for a more sustained release of the nanoparticles in order to improve the transfection efficiency[72]. Recently a layer by layer technique [91, 95-97] was used to immobilize PEI and DNA on the surface of electrospun scaffold for gene delivery. Using this technique, the loading efficiency of several μg DNA per mg scaffold was obtained and significant enhancements in wound healing were produced[91]. This technique can also be applied to this study to improve the loading efficiency of the DNA so as to enhance the transfection efficiency and overall sustained release.

Aside from the improvement of gene delivery efficiency, the tissue engineering scaffold itself needs to be fully studied for its osteoconductivity/biocompatibility. Although previous studies in our laboratory has already demonstrated that the collagen/PLLA scaffold is favorable for cell attachment, migration, proliferation and differentiation of osteoblasts, the degradability property of the scaffold is still not

determined, which is a very important property for supporting bone formation. The degradation rate of a bone tissue engineering scaffold is expected to be the same as the generation rate of new bone so that the implant does not impede the formation of the new bone [93, 98]. In this study, we did observe some break down of the scaffold after 4 weeks of implantation (as shown in the histological images), but the degradation needs to be evaluated more quantitatively and for a longer time period, both *in vitro and in vivo*.

To combine the gene delivery system and tissue engineering scaffold together, generally two strategies can be used: to absorb the transfection complex on the surface of the scaffold or to include the complexes inside the electrospun fibers. In this study, the complexes were adsorbed on the surface of the scaffold and showed great ability to transfect the surrounding tissue of the scaffold. However, the lack of enough mineralization and bone production in the later time points may indicate that the release of the transfection complexes needs a more sustained profile to generate consistent production of the rhBMP2 protein for effective bone induction[99], considering that the delivery of a single dose of rhBMP-2 plasmid can only incur transient transfecion and gene expression. Since bone formation occurs through a series of sequential, well-defined steps, a transient expression of rhBMP-2 may provide inadequate levels at critical steps in the bone formation cascade. Furthermore, *in vivo* degradation and dilution of rhBMP-2 may render significant decrease of tissue concentration [89]. Inclusion of the transfection complexes into the polymer solution for electrospining may provide a way for protection as well as sustained release of the transfection complexes

[99] since some of the transfection complexes inside the electrospun fibers can only be released upon the degradation of the scaffold, which may have a time span of a few weeks. In the future, the combination of these two means of immobilization can be explored for more suitable rhBMP2 protein production profile.

The background of the x-gal staining may come from endogenous β-gal activity according to previous studies by other researchers [100-102]. It was reported that endogenous β-gal and its several different isozymes presented in many mammalian cells and tissues including skeletal muscles. Using a weakly alkaline pH during the staining, the endogenous β-gal activity could be minimized. However, most published protocols described X-gal staining at a neutral pH, which may not allow differences between endogenous and exogenous enzyme activities [100]. This study also used a neutral pH in the X-gal staining following our previous protocol [33], and this condition probably caused the high background. Further studies are needed to be performed in order to find out if the change of pH to a weakly alkaline one can eliminate the background. If the issue cannot be resolved, other reporter genes can be used to detect the transgene expression.

The signaling process of BMP2, which has not been understood completely, generally includes canonical (Smad dependent) pathway and non-canonical (Smad-independent) pathways [103, 104]. The canonical pathway is initiated when BMP2 binds to its type I and type 2 receptors and then Smads 1, 5 or 8 are phosphorylated and complex with Smad 4. These complexes travel to the nucleus and regulate target gene

transcription including Runx2, Osterix, Oscteocalcin, type I Collagen, Osteopontin etc. Other signaling pathways, such as MAPK and ERK etc, were also reported to be involved in the BMP2 signaling as a non-canonical pathway for induction of osteoblastic differentiation of mesenchymal progenitor cells [105]. Transcription factor Runx2 is one of the target genes of BMP2 signaling and plays a essential role in osteoprogenitor cell differentiation/bone formation[106-108]. Type I collagen is the most abundant extracellular matrix protein and is essential for bone strength[106]. Osterix was reported as a transcription factor downstream of Runx2 regulating osteoblast differentiation [109]. Osteocalcin is a bone matrix protein for Ca^{2+} binding [110]. They are both markers of osteoblast differentiation/bone formation[108]. In this study, the mRNA level of all these genes were found not to be upregulated or detectable on both day 3 and day 7 after BMP2 scaffold implantation, even though strong rhBMP2 mRNA and protein expression was detected by IHC at day 7, indicating that either the expressed rhBMP2 protein could not induce effective signal transduction on the surrounding cells of the scaffold or the time points tested were not appropriate for the rhBMP2 signaling events to be observed. It was reported that the maximum mRNA level of Runx2 was detected 2hrs after 300ng/ml of BMP2 stimulation on C2C12 cells *in vitro* and it returned to the original levels after 24 hrs of stimulation [106]. Thus, the latter possibility may be the real case since it can explain the identification of some mineralization on day 14 and day 28. Measurement of the expression of these osteogenic marker genes at additional time points would be one way to resolve this issue.

The mineralization/bone formation observed through radiography and histology was consistent. It is notable that on day 14, there was also some mineralization in the "scaffold only" group. This ossification may be resulted from the injury of the surgery since it is known that traumatic injury can cause heterotopic ossification [111]. However, on day 28, mineralization was not found in the "scaffold only" control group. Obviously in future experiments, the BMP2 gene delivery efficiency needs to be improved so that the mineralization/bone formation can be strong enough to be clearly distinguished from the negative control.

4.4 Conclusion

BMPs have been discovered about 50 years ago and their prominent property of augmenting bone formation has been applied to clinic for the treatment of bone fractures, nonunions and spine fusion. However, BMPs were only used in protein form clinically and the high dose of administration increases the cost and the burst release of the protein incurred unwanted side effects [112]. Gene delivery of BMPs may circumvent these disadvantages and has attracted a lot of research interest. Various gene delivery techniques can be used to apply BMP gene therapy to skeletal disorders. Among these techniques, non-viral gene delivery systems using polymer based vectors are much safer than viral vectors and the combination with tissue engineering scaffolds can provide more availability to these delivery vehicles and to the surrounding cells because the scaffold can be designed to support cell migration, proliferation, and differentiation. Using an electrospun scaffold to deliver BMP genes represents a novel approach to bone-healing augmentation. Potential clinical applications for this approach to augment bone formation include fractures, delayed and nonunions, bone defects,

spinal fusions, peripheral joint arthrodeses, oncologic skeletal reconstructions, and bone ingrowth into joint arthroplasty prostheses,etc. In this specific aim, the feasibility of using electrospun Collagen/PLLA scaffold with surface immobilized rhBMP2 transfection complex gene delivery system to induce bone formation was established. Therefore, this study represents an important first step in the development of an eletrospun Collagen/PLLA scaffold combining gene therapy with BMP-2. However, although promising, additional research is needed before clinical application can be achieved.

Table 1. Final summary of animal experiments.

	Time Points			
Group	Day 3	Day 7	Day 14	Day 28
1. "scaffold only" total 12 animals -Negative Control	4 animals 2 for X-gal &IHC, 2 for PCR	4 animals 2 for X-gal & IHC 2 for PCR	2 animals µCT, histology	2 animals µCT, histology
2. "scaffold + β-gal complexes" total 7 animals -Control	2 animals X-gal	1 animals X-gal	2 animal µCT, histology	2 animals µCT, histology
3. "scaffold+BMP2 complexes" total 12 animals - Experimental	4 animals 2 PCR, 2 IHC	4 animals 2 PCR, 2 IHC	2 animals µCT, histology	2 animals µCT, histology
4. "BMP2 complexes injection" total 8 animals - Experimental	2 animals for PCR bad RNA extraction	2 animals for PCR bad RNA extraction	2 animals µCT, histology	2 animals µCT, histology
5. "scaffold+BMP2 protein" total 5 animals -Positive Control	1 animal for IHC		2 animals µCT, histology	2 animals µCT, histology

Note: Orininally each analysis of all groups started with 2 animals but due to some negligence when conducting the experiment, some animals died.

Figure 1. Position of the muscle pouch created on the gracilis and muscles from lateral aspect of the left hip, thigh and lower leg of mouse with the superficial layer of muscles removed. Cranial surface to the right. [78]

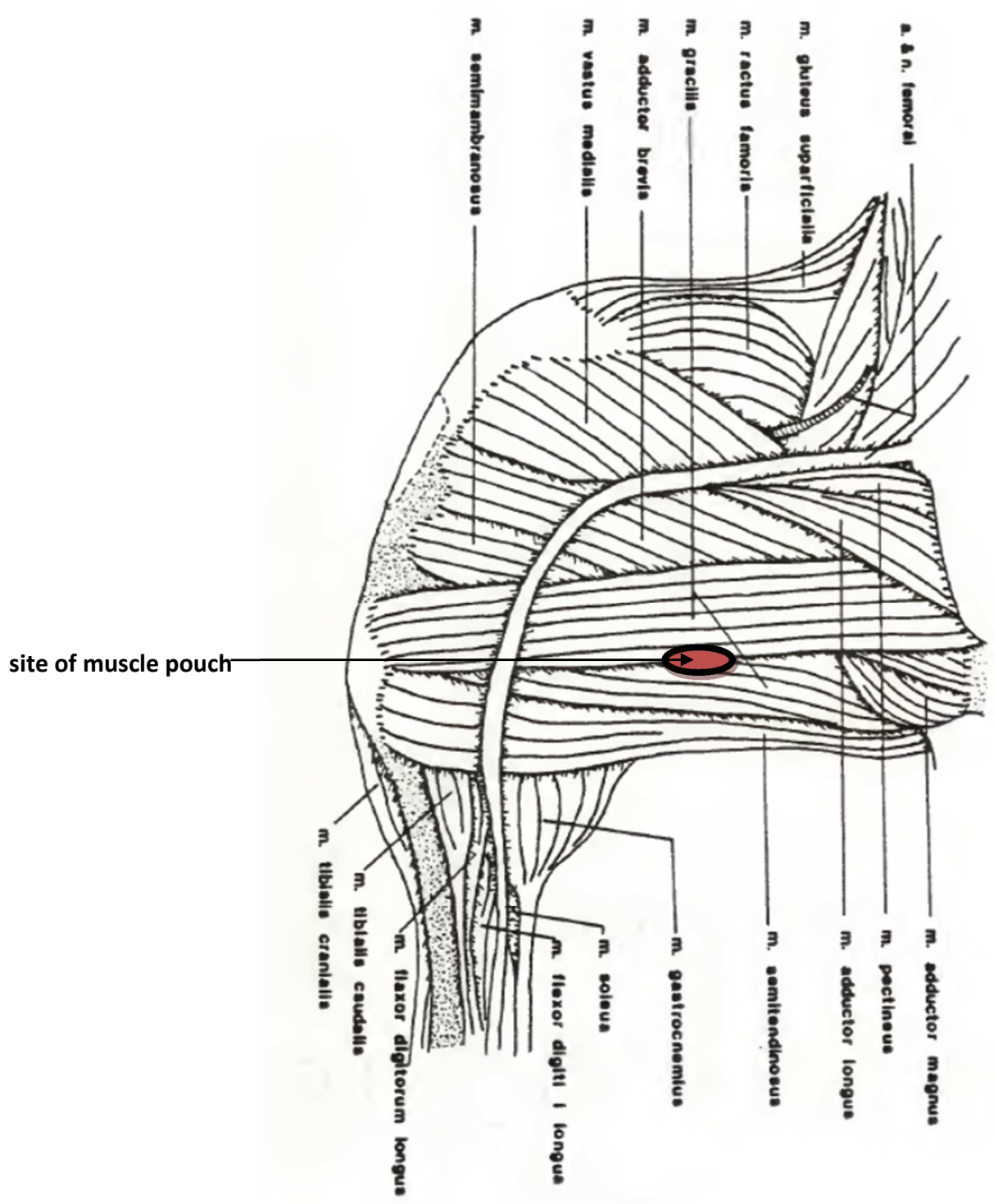

Table 2. Real-time PCR primer sequences

Gene	Access number (Gene bank)	Forward primer sequence	Reverse primer sequence
hBMP2	NM_001200	GGCATCCTCTCCACAAAAGA	AGCCACAATCCAGTCATTCC
mRUNX2	NM_001146038.2	AGCAGCACTCCATATCT	CTTCCGTCAGCGTCAA
mCOL1A1	NM_007742.3	CTGGCAAGAATGGCGA	GAAGCCACGATGACCC
mOSC	NM_007541.2	CCATCTTTCTGCTCACTCTGC	ACCTTATTGCCCTCCTGCTT
mOSX	AY803733.1	AGGCACAAAGAAGCCATACG	GGGAAGGGTGGGTAGTCATT
mGAPDH	BC083080	ACCAACTGCTTAGCCC	CTTCCCGTTCAGCTCT

Table 3. summary of X-gal staining result.

	positive	negative	total	Positive rate
Scaffold only day 3	2	2	4	50%
Scaffold+β-gal complex day 3	4	0	4	100%
Scaffold only day 7	3	1	4	75%
Scaffold+β-gal complex day 7	2	0	2	100%

Figure 2. β-galactosidase activity resulting from β-gal delivery via the electrospun scaffold. (A, B) Low and high magnification image of X-gal staining of "scaffold only" group of a day 3 sample showing background blue staining surrounding the scaffold. (C,D) Low and high maginification image of X-gal staining of "scaffold+β-gal complexes" group on day 3 also showed blue staining surrounding the scaffold. (E, F) Low and high magnification image of the "scaffold only" group of a day 7 sample showing background blue staining surrounding the scaffold. (G, H) Low and high magnification image of the "scaffold +β-gal complexes" group on day 7 showing blue staining surrounding the scaffold.

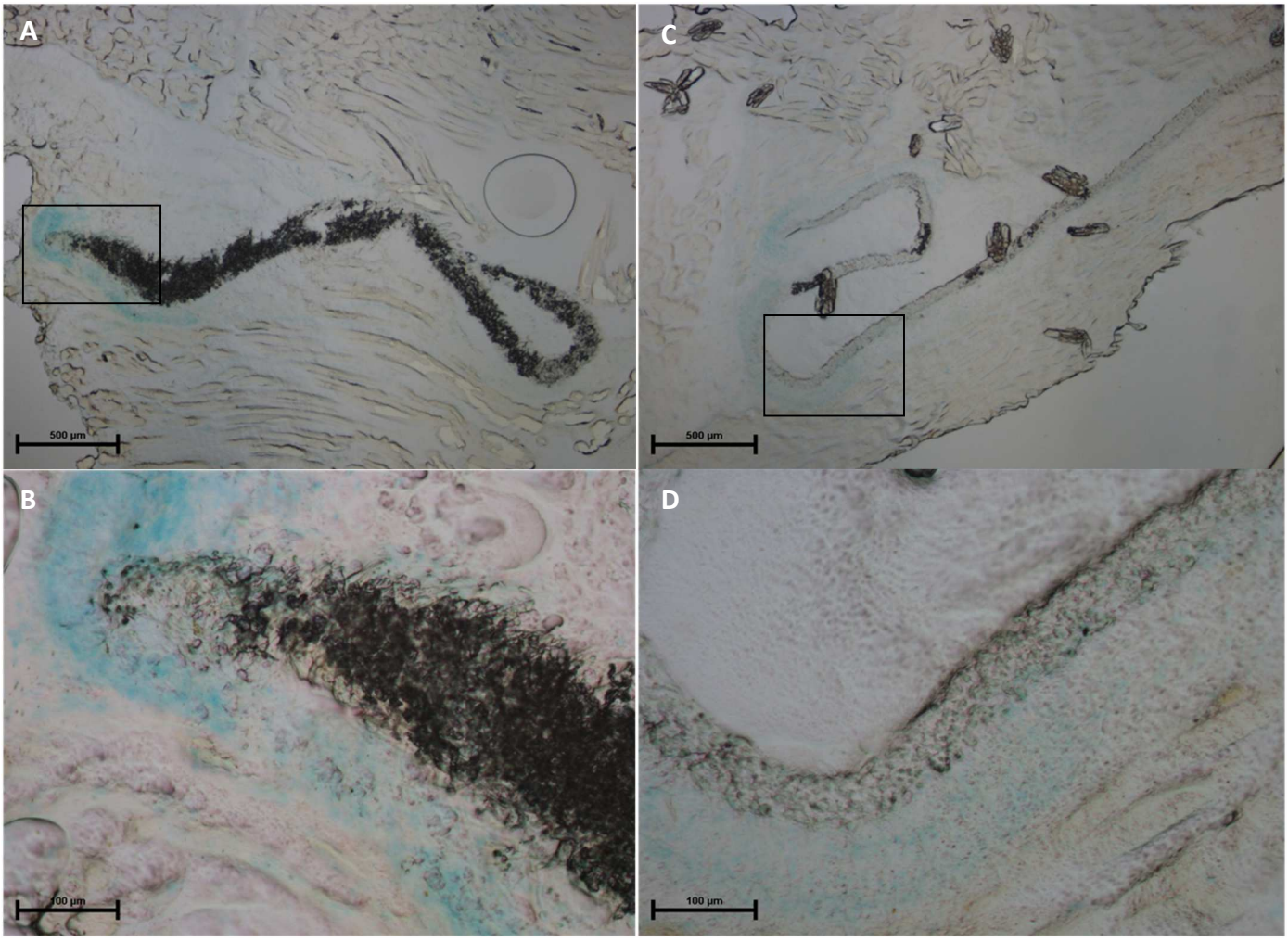

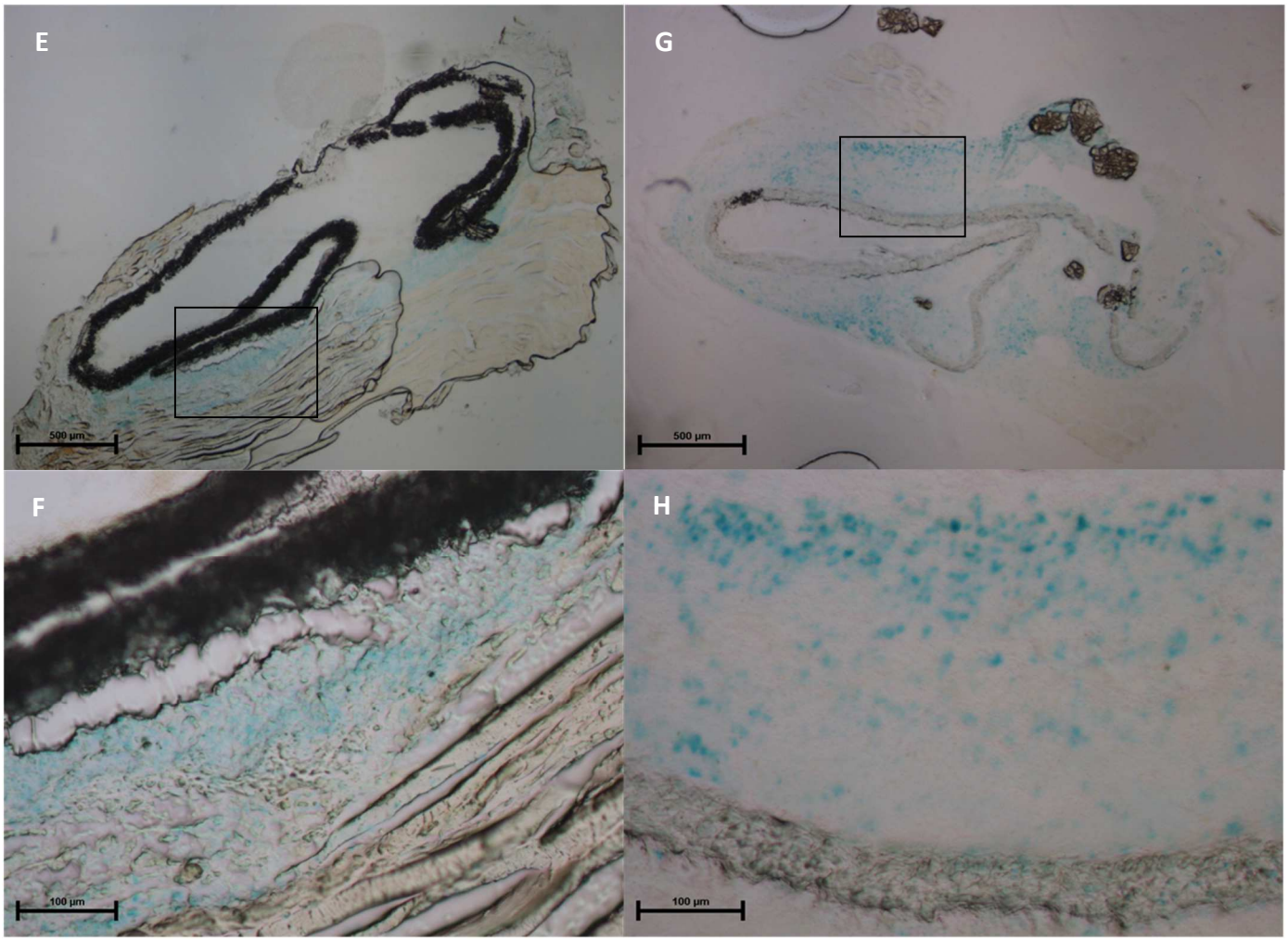
E
500 µm
G
500 µm
F
100 µm
H
100 µm

Figure 3. Quantitative real time PCR analysis (A) rhBMP2, (B) mRUNX2 and (C) mCOL1A1 mRNA level on day 3 and day 7 of implantation. The "scaffold only" group served as control and was normalized to 1. * represents $p<0.05$ comparing to control.

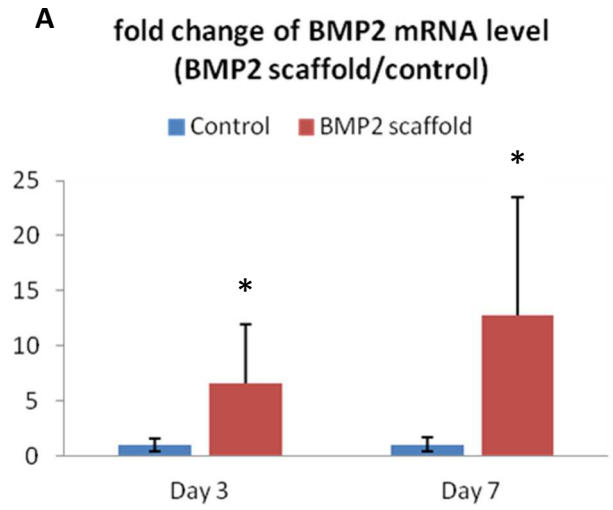

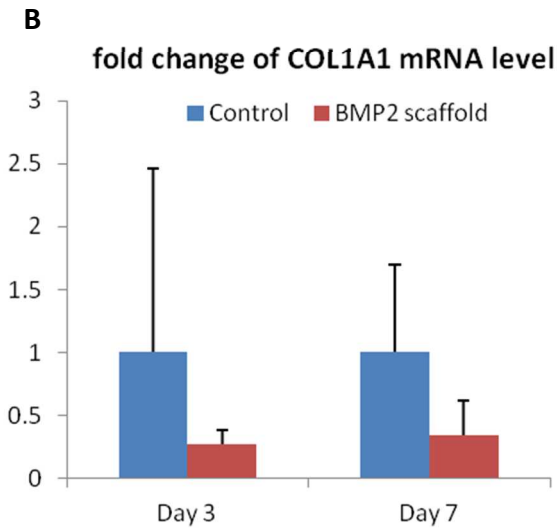

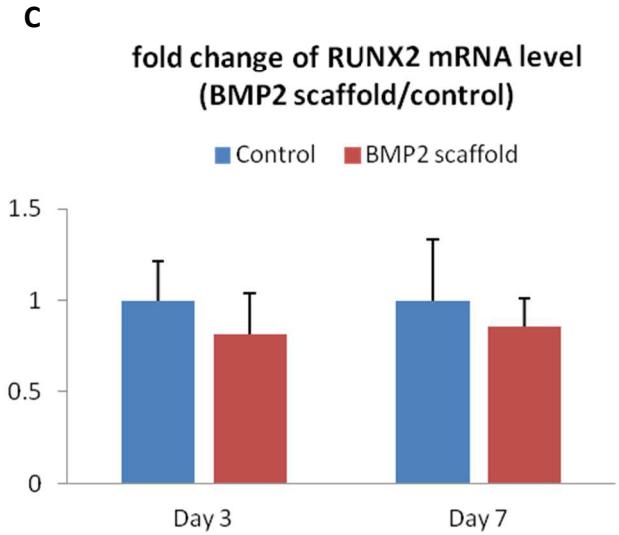

Table 4. Summary of immunohistochemisty of rhBMP2

	Positive	Negative	Total	Positive rate
Scaffold only day 3	0	4	4	0%
Scaffold+BMP2 complexes day 3	0	4	4	0%
Scaffold+ BMP2 protein day 3	0	2	2	0%
Scaffold only day 7	1	3	4	25%
Scaffold+BMP2 complexes day 7	4	0	4	100%

Figure 4. Immunohistochemistry of rhBMP2 protein expression. Low/high magnification images of typical day 3 samples of "scaffold only" (A/B), "scaffold+BMP2 complexes" (C/D) and "scaffold+BMP2 protein" (E/F) groups showed no staining of rhBMP2 protein. Low/high magnification images of a typical day 7 sample of "scaffold only" (G/H) group showed no staining of rhBMP2 protein. Low/high magnification images of a tyical day 7 sample of "scaffold+BMP2 complexes" group (I/J) demonstrated red rhBMP2 staining surrounding the scaffold.

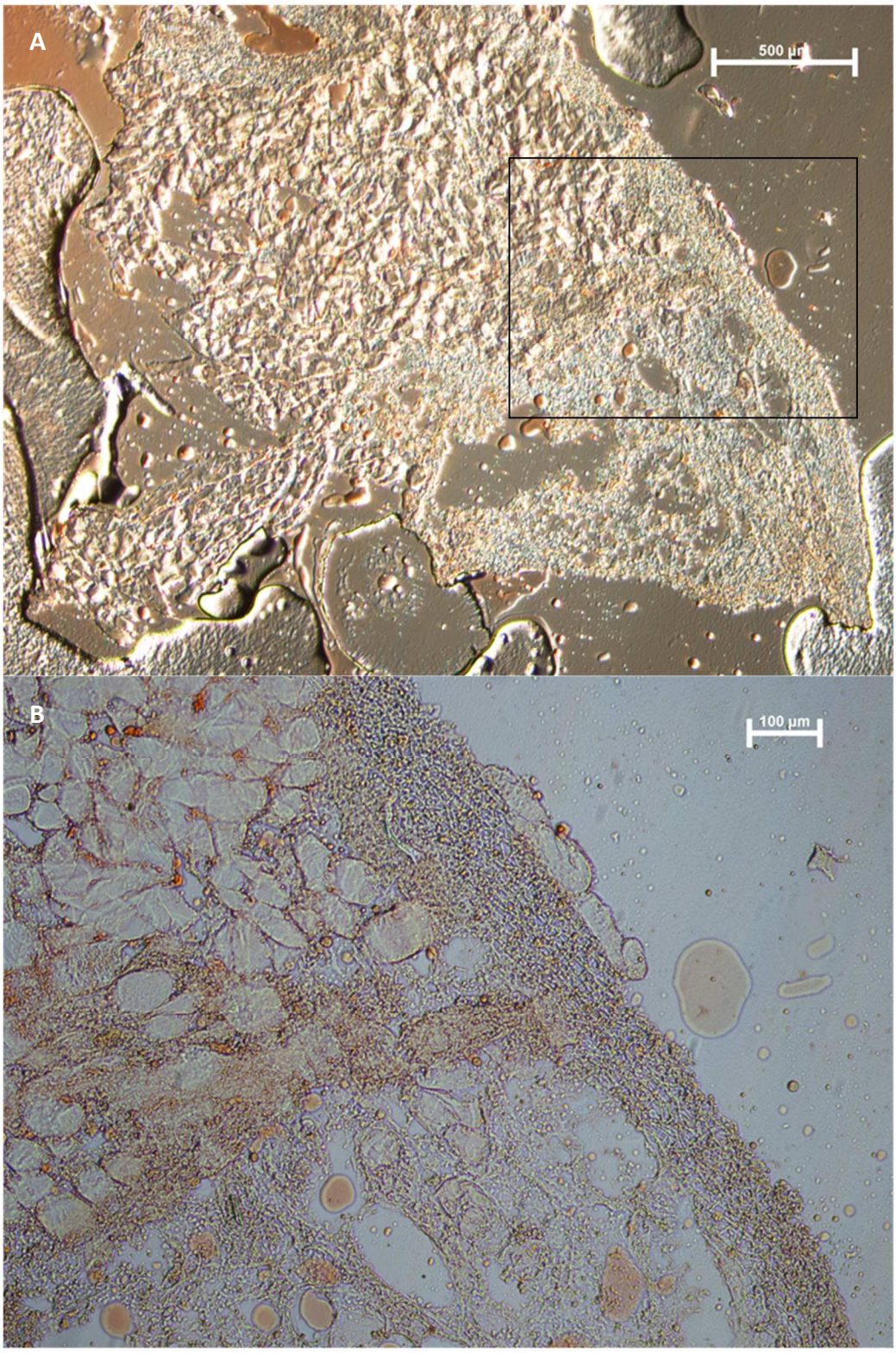
A
500 µm
B
100 µm

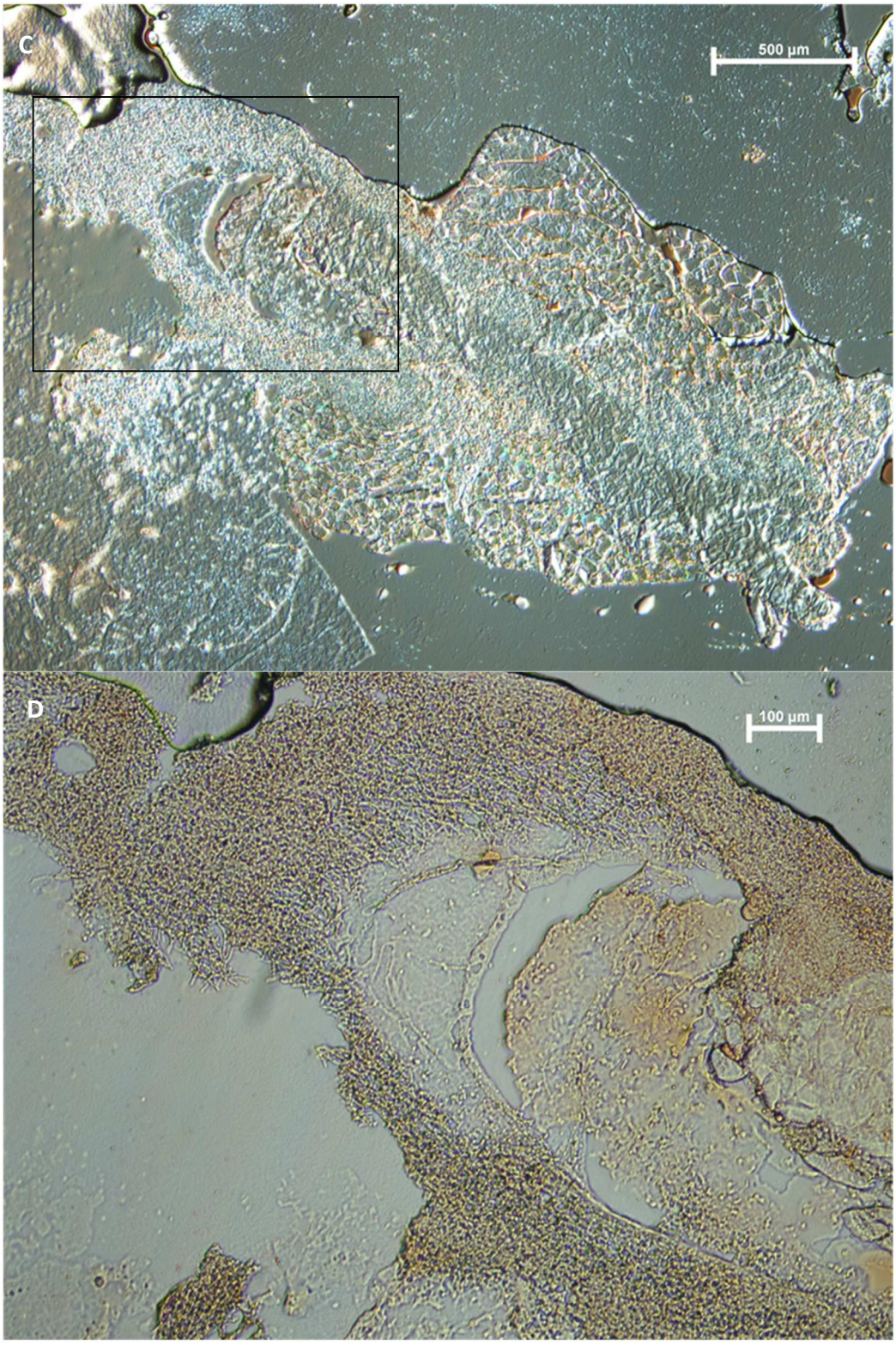
C
500 µm
D
100 µm

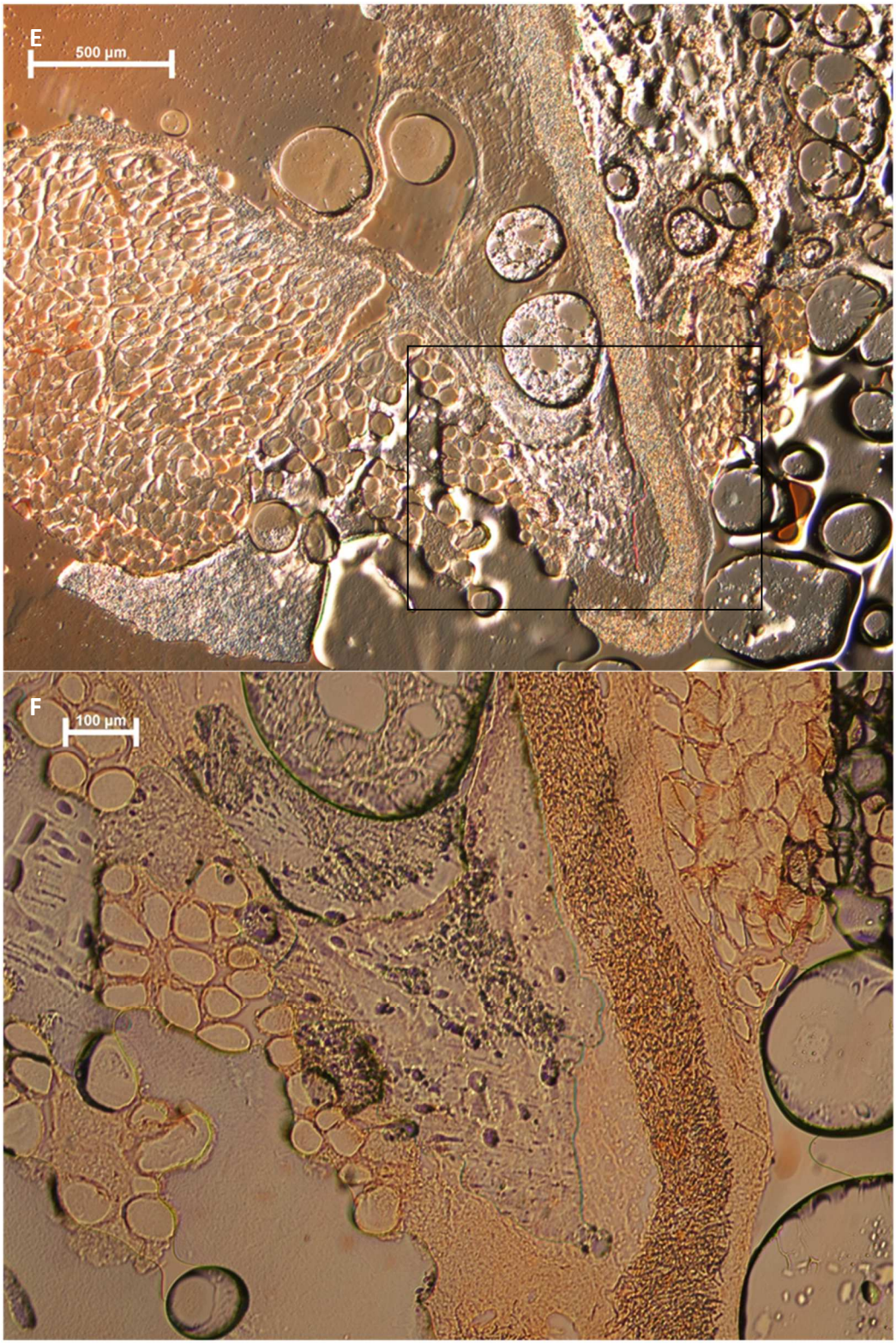
E
500 µm
F
100 µm

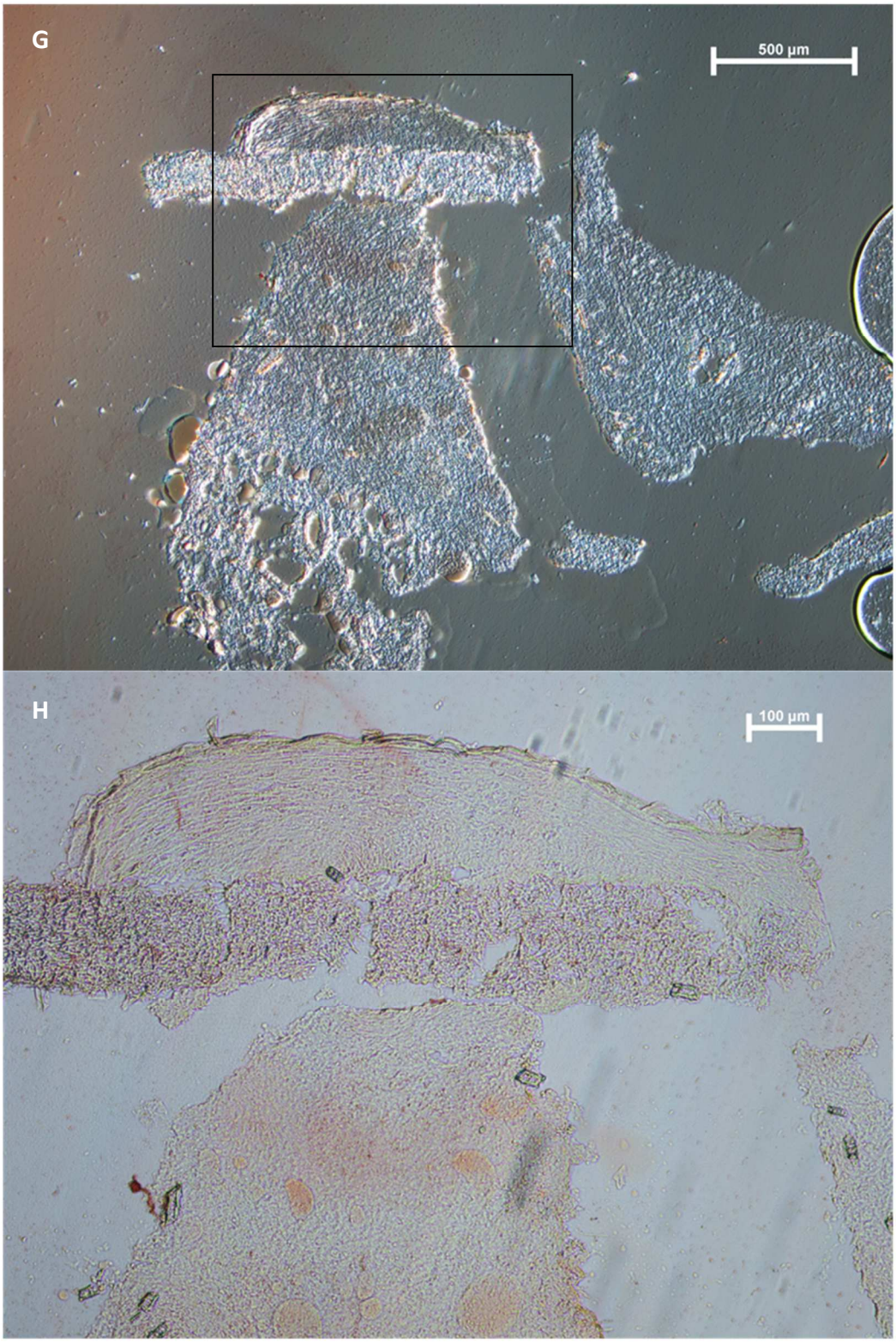
G
500 µm
H
100 µm

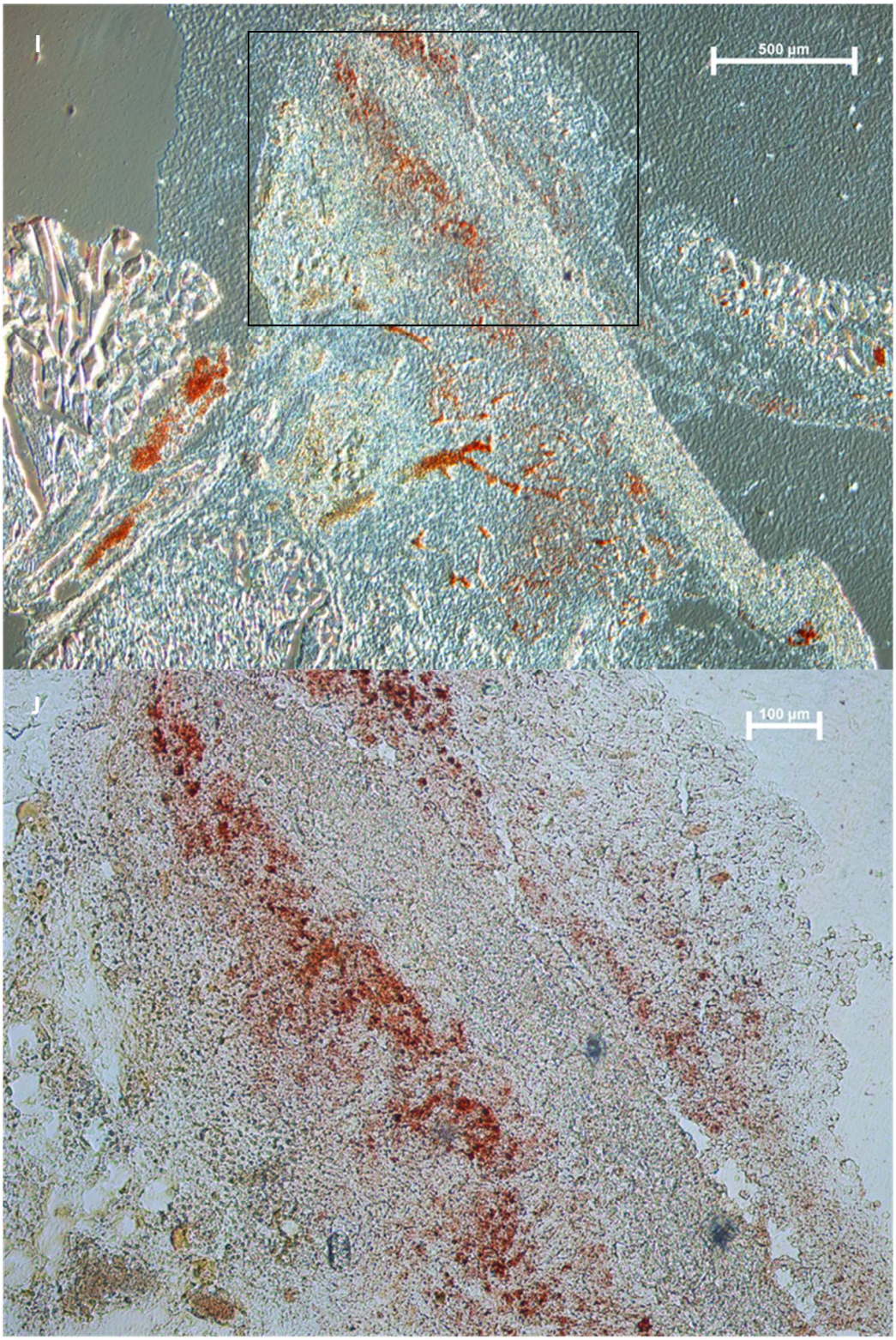
I
500 µm
J
100 µm

Figure 5. BV/TV ratio of day 14 and day 28 samples.

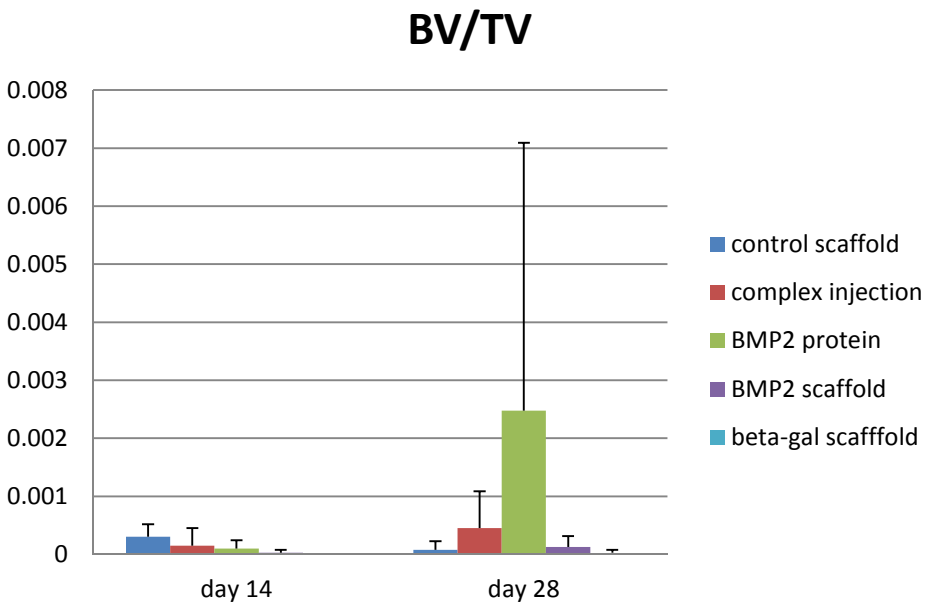

Table 5. Summary of Alizarin red staining of day 14 and day 28 specimens.

	Positive	Negative	Total	Positive rate
Scaffold only day 14	1	3	4	25%
Scaffold+β-gal complex day 14	0	4	4	0
Scaffold+ BMP2 complex day 14	1	3	4	25%
BMP2 complex injection day 14	0	4	4	0
Scaffold+BMP2 protein day 14	3	1	4	75%
Scaffold only day 28	0	4	4	0
Scaffold+β-gal complex day 28	0	4	4	0
Scaffold+ BMP2 complex day 28	3	1	4	75%
BMP2 complex injection day 28	0	4	4	0
Scaffold+BMP2 protein day 28	1	3	4	25%

Figure 6.Mineralization after day 14 and day 28 of transfection detected by Alizarin red staining. (A-I) Alizarin red staining of day 14 specimens. (A) "scaffold only" group. (B) "scaffold+β-gal complexes" group. (C-E) Scaffold+BMP2 complexes" group under different magnification. (F) "BMP2 complex rejection" group. (G-I) "scaffold+BMP2 protein" group. (J-Q) Alizarin red staining of day 28 specimens. (J) "scaffold only" group. (K) "scaffold+β-gal complexes" group. (L, M) Scaffold+BMP2 complexes" group under different magnification. (N) "BMP2 complex rejection" group. (O-Q) "scaffold+BMP2 protein" group. Arrow: mineralization.

Day 14 scaffold only

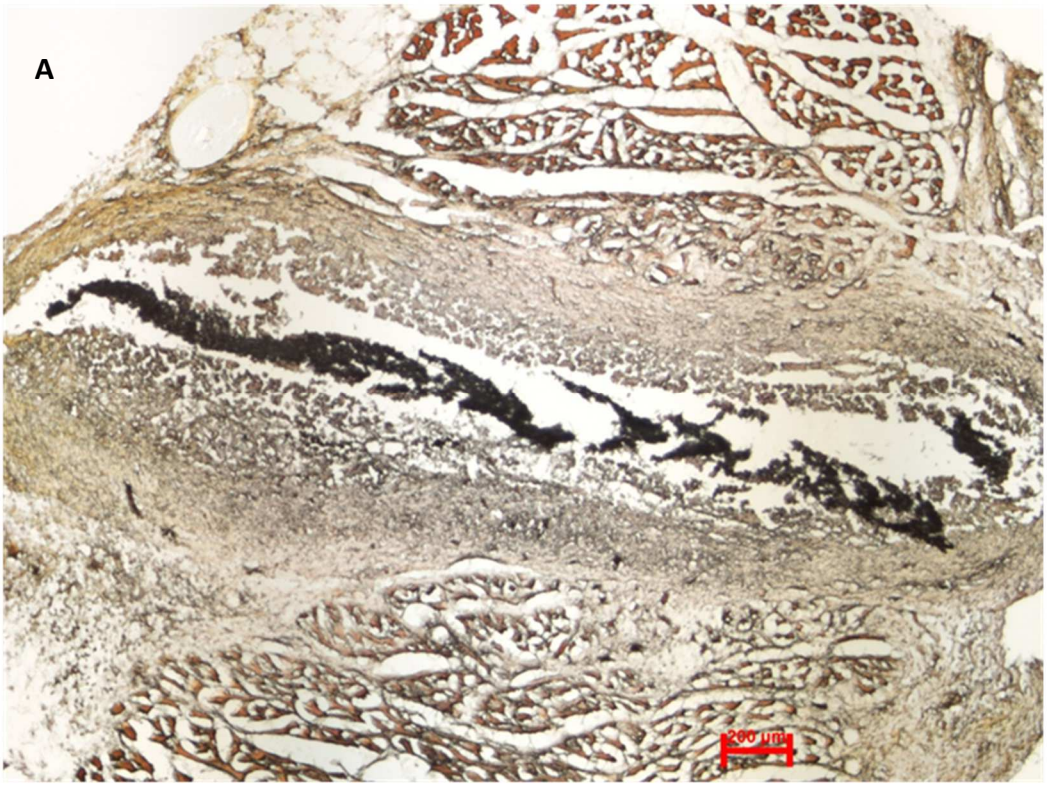

Day 14 scaffold + β-gal complex

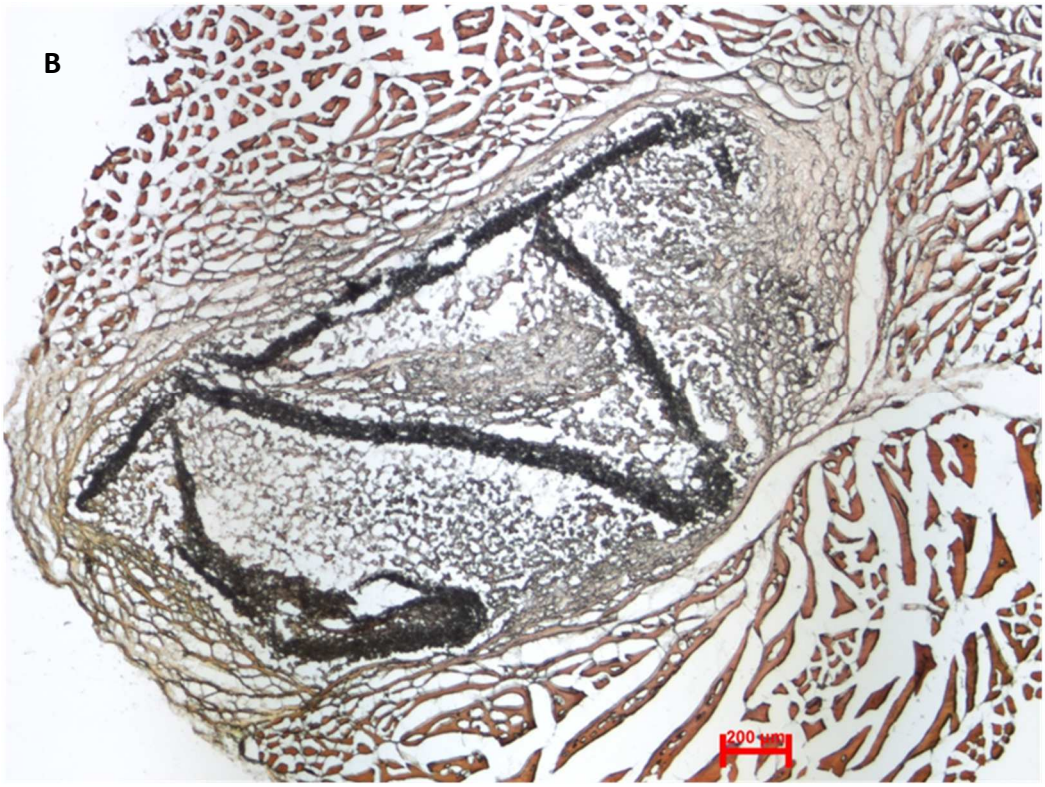

Day 14 scaffold+BMP2 complex

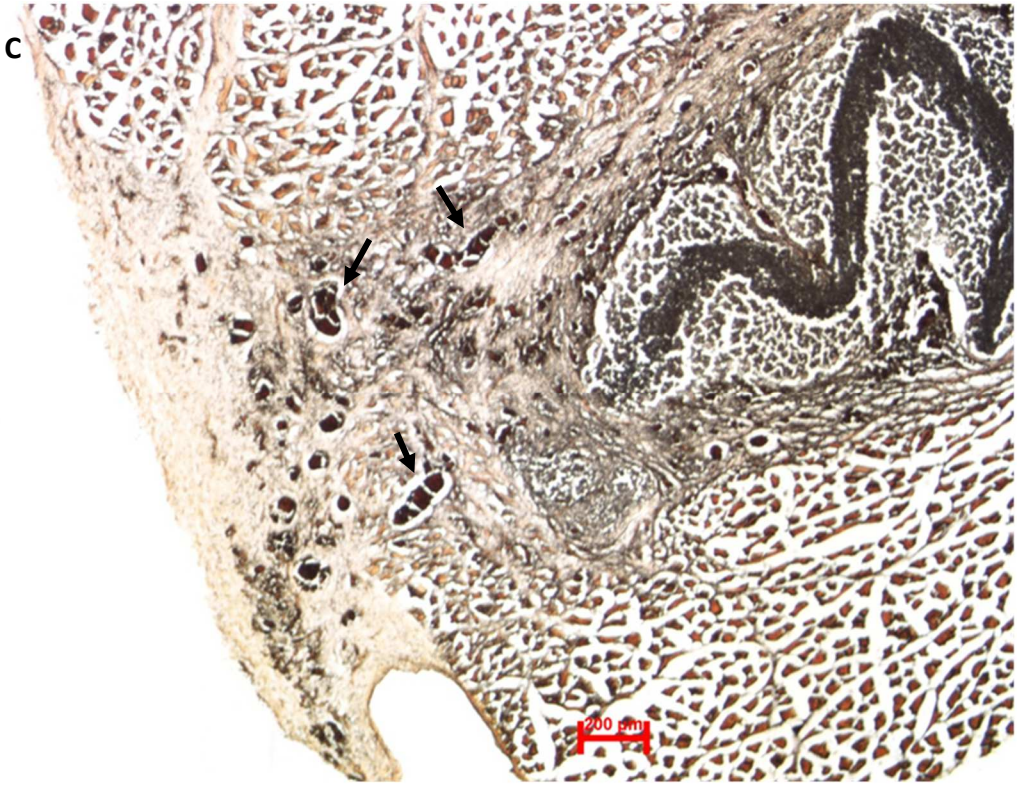

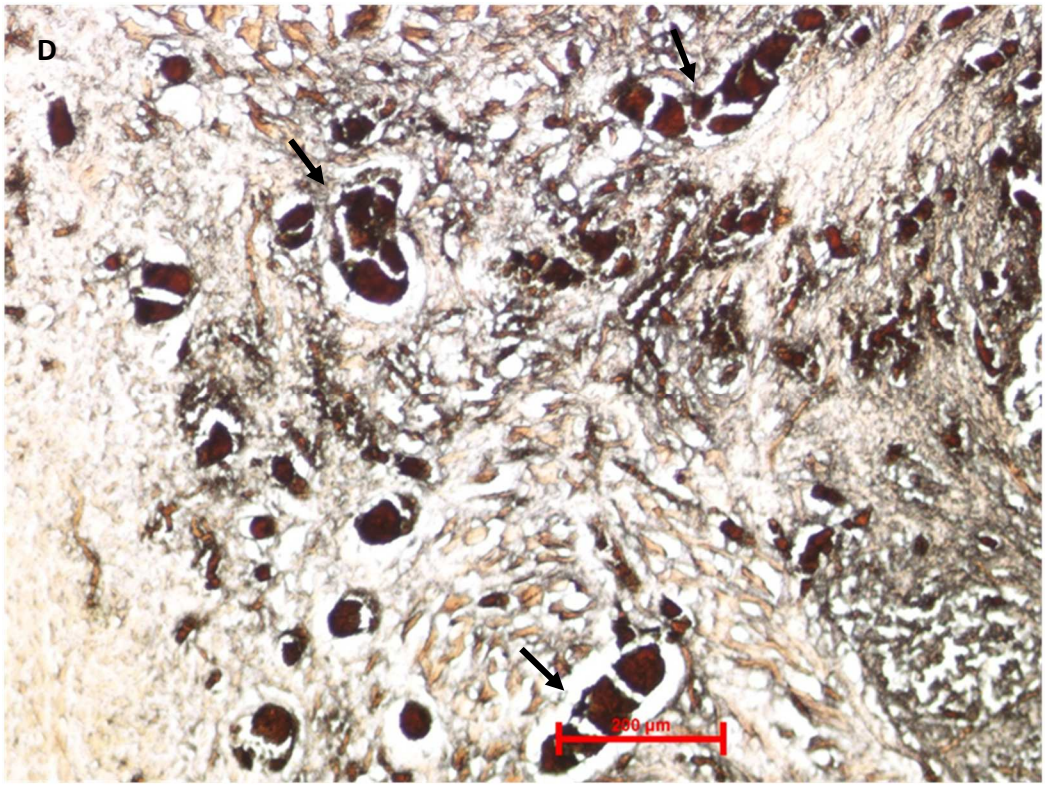
D
200 µm

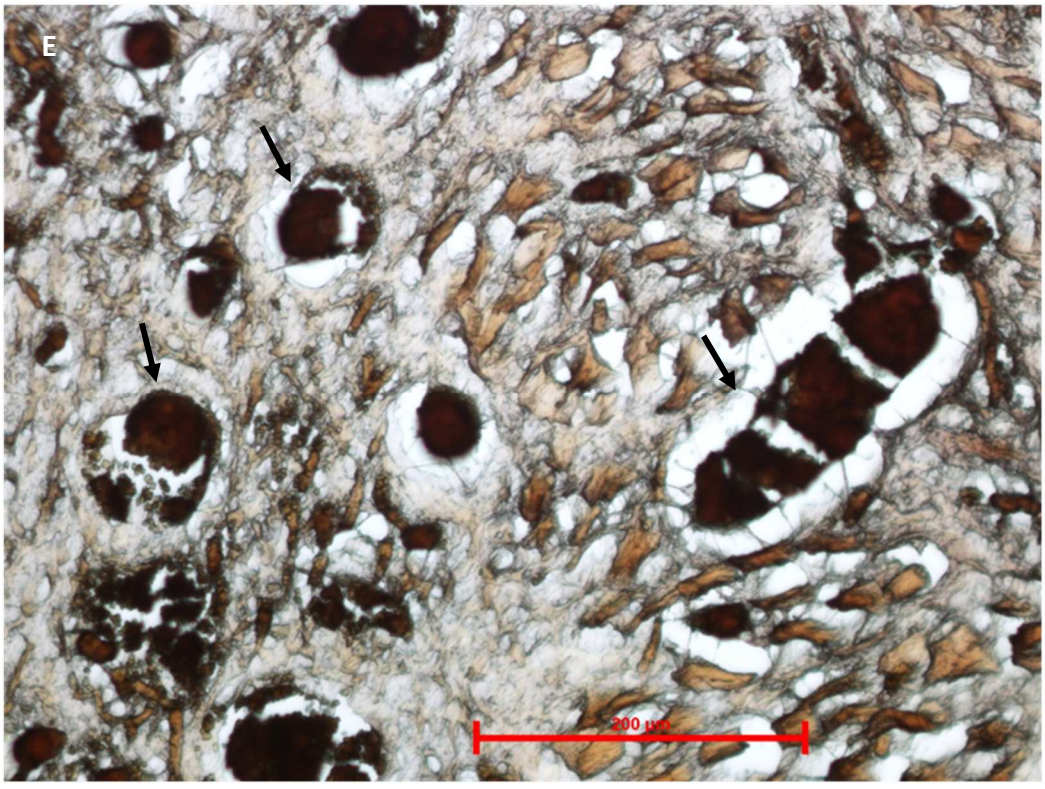
E
200 µm

Day 14 BMP2 complex injection

Day 14 scaffold + BMP2 protein

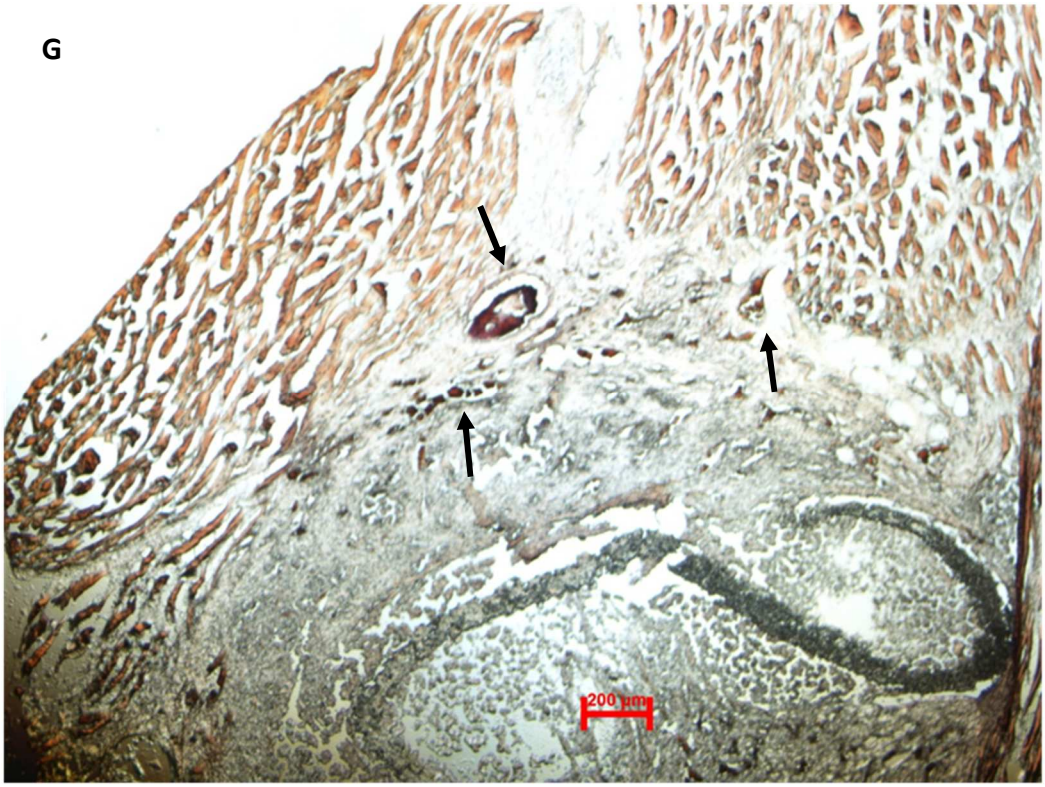


H
200 µm

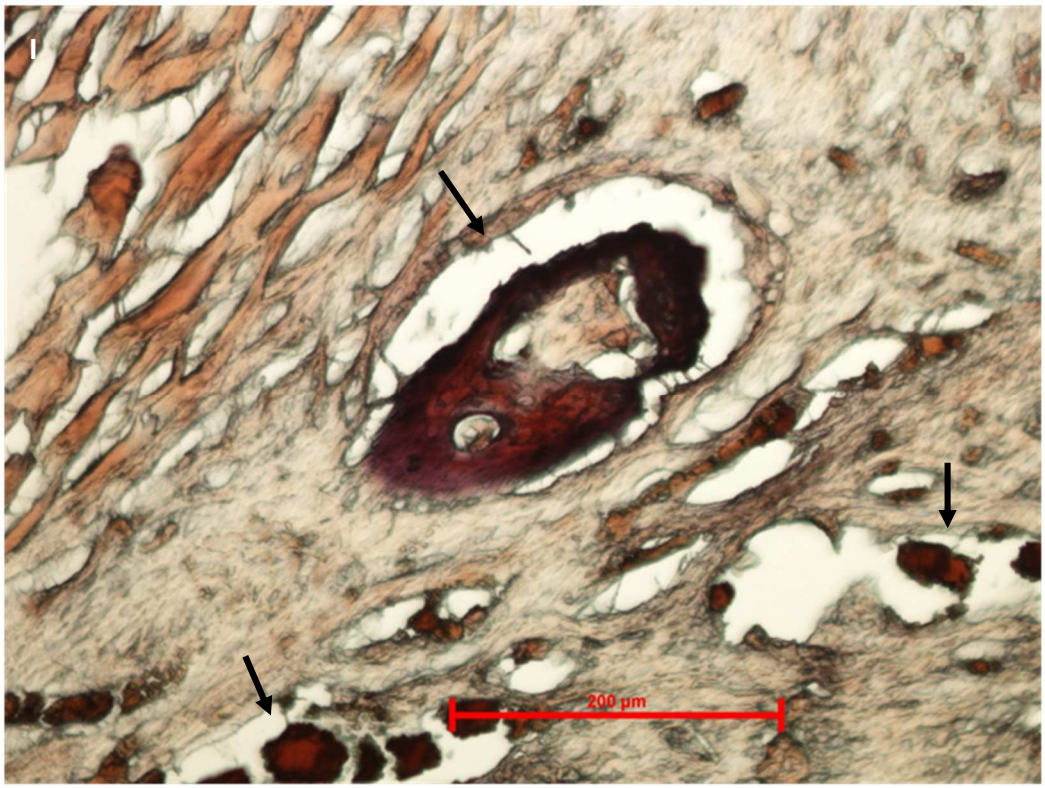
I
200 µm

Day 28 scaffold only

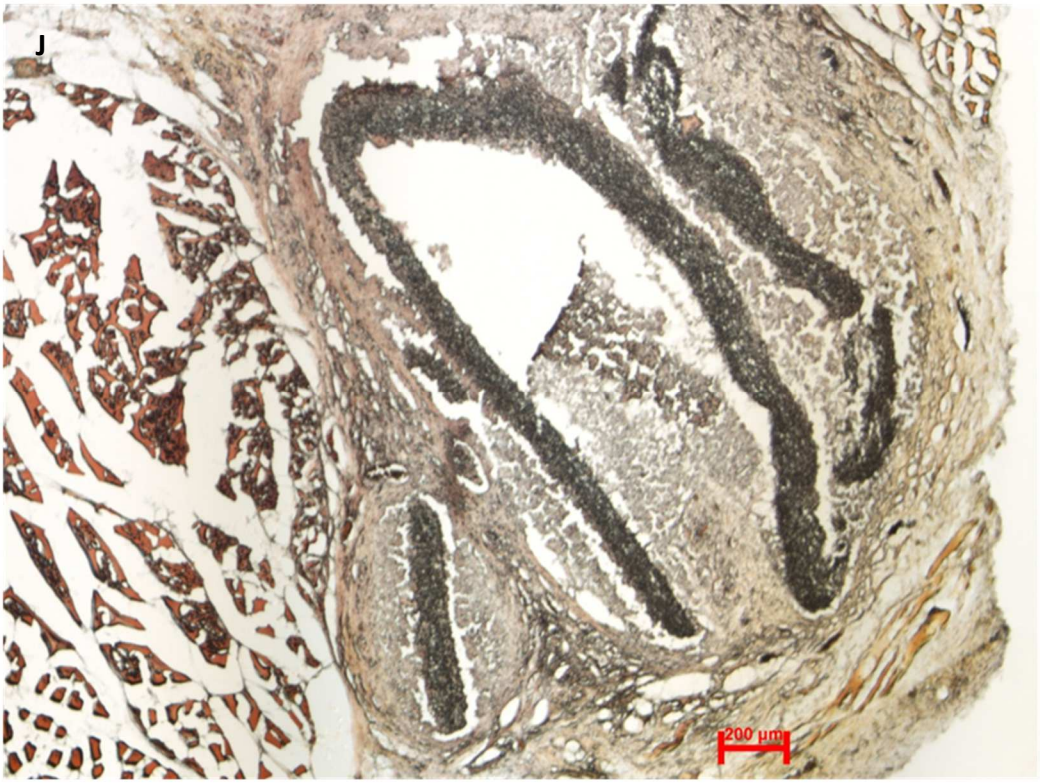

Day 28 scaffold + β-gal complex

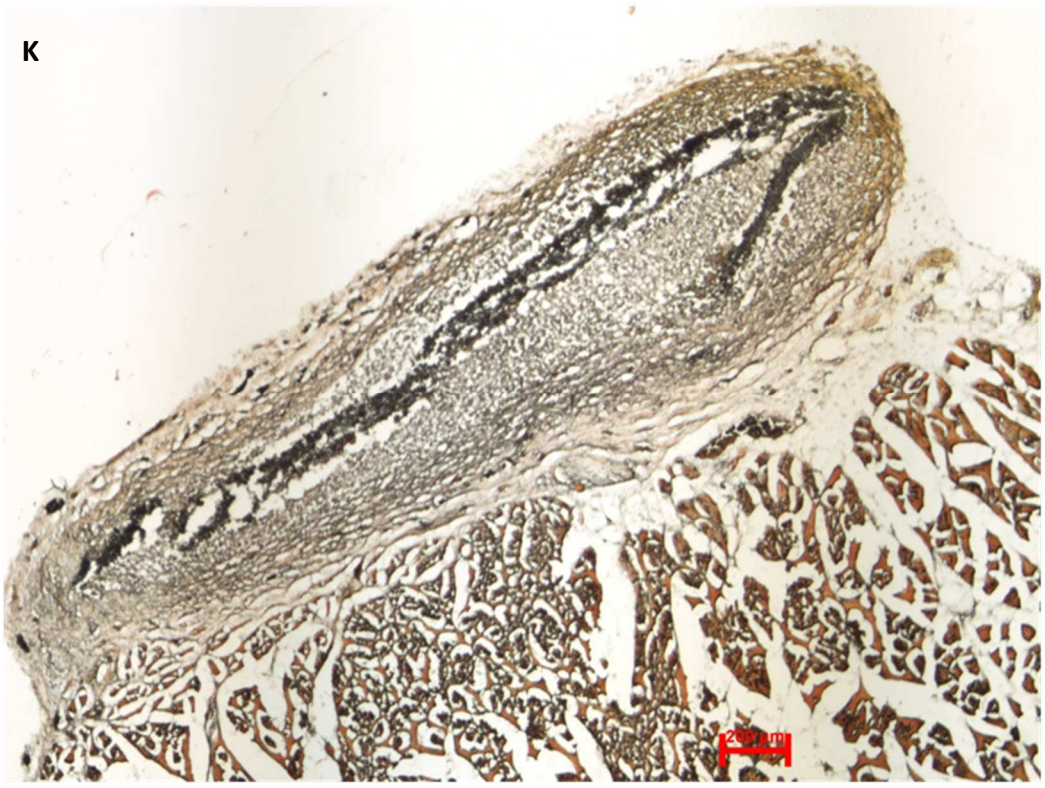

Day 28 scaffold+ BMP2 complex

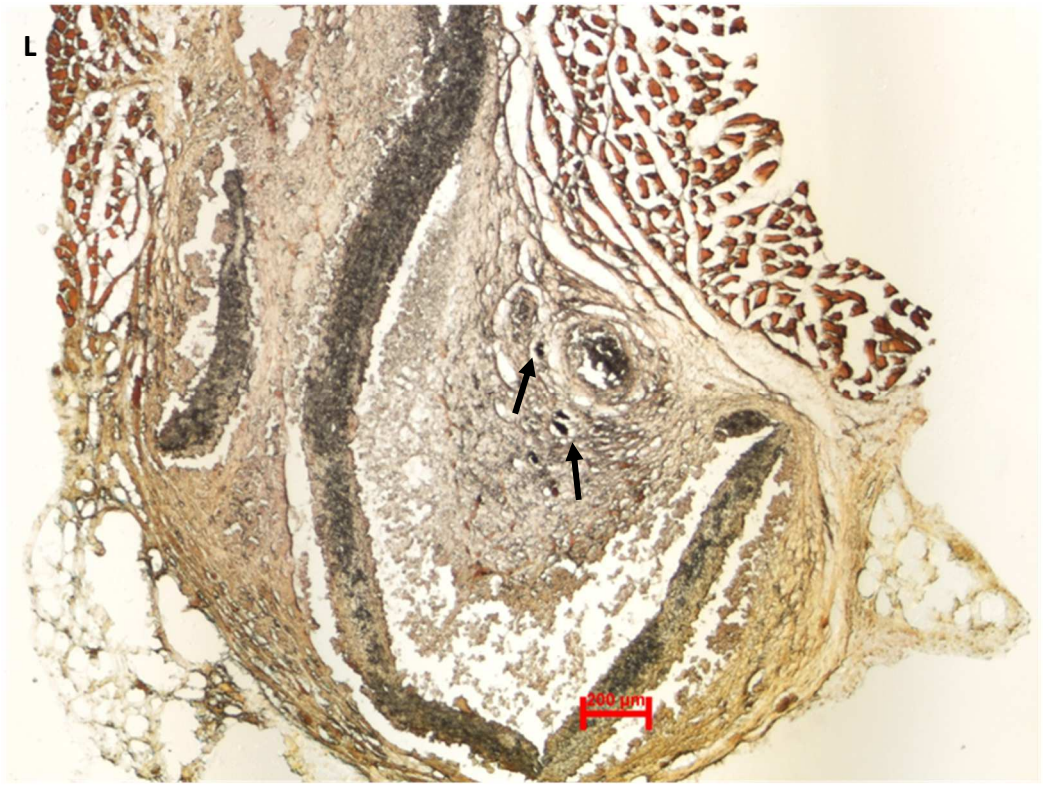

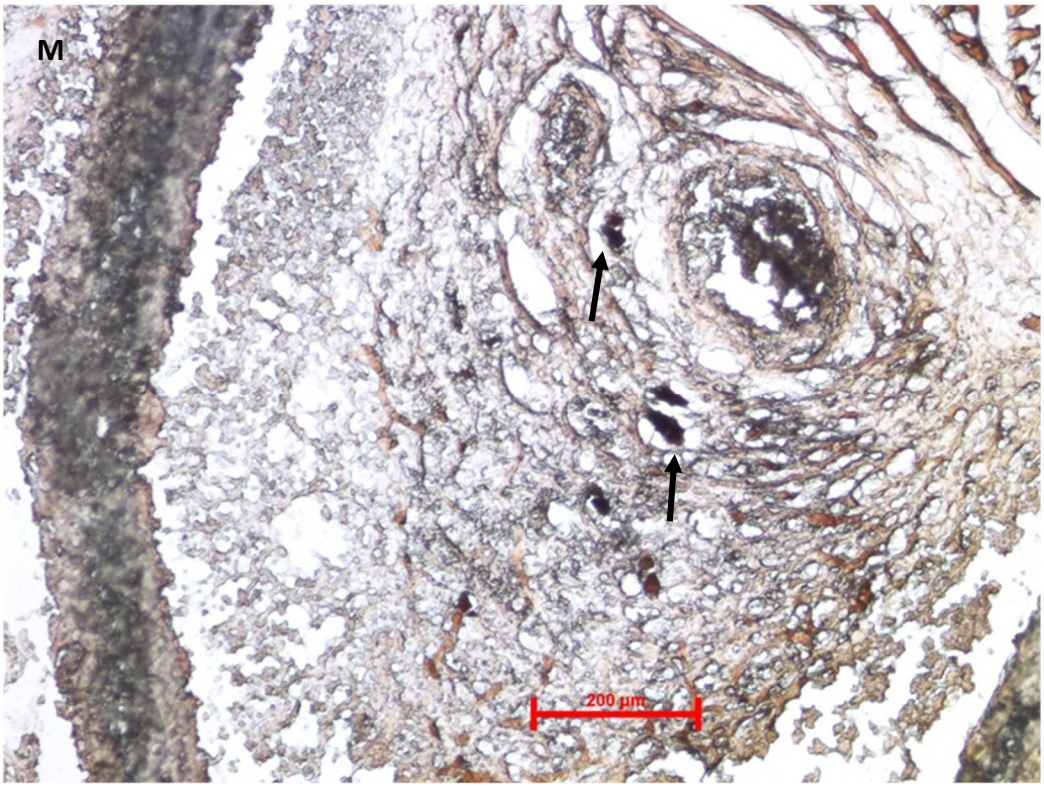

Day 28 BMP2 complex injection

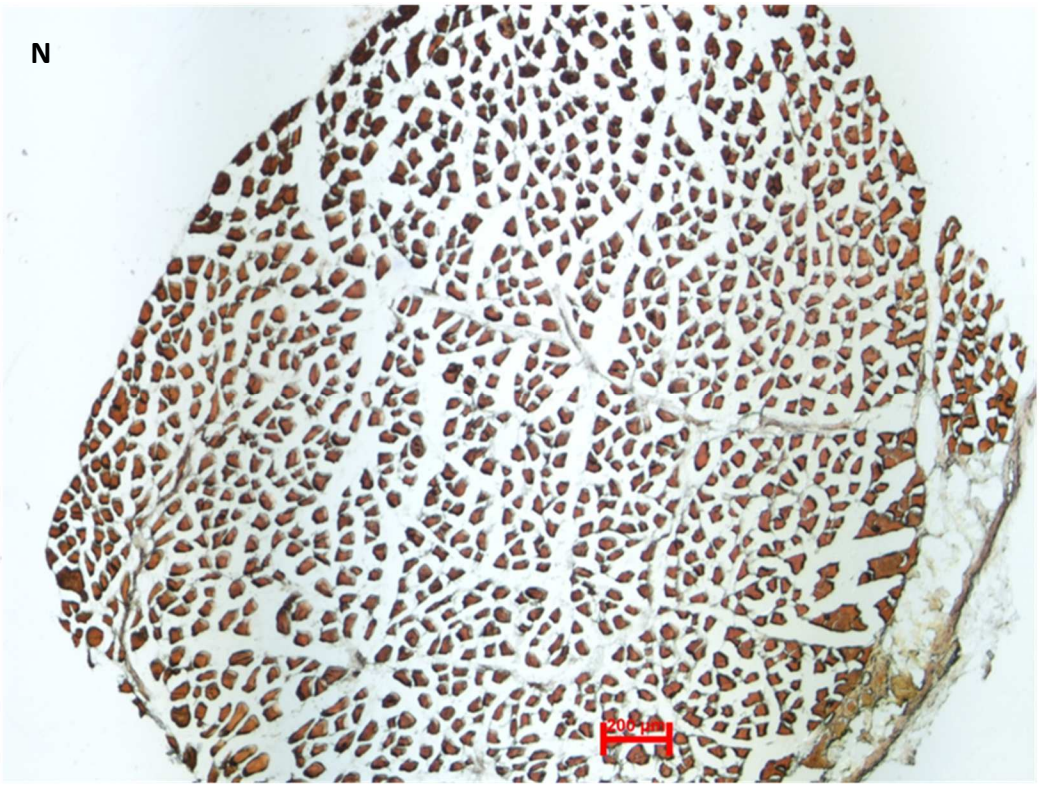

Day 28 scaffold + BMP2 protein

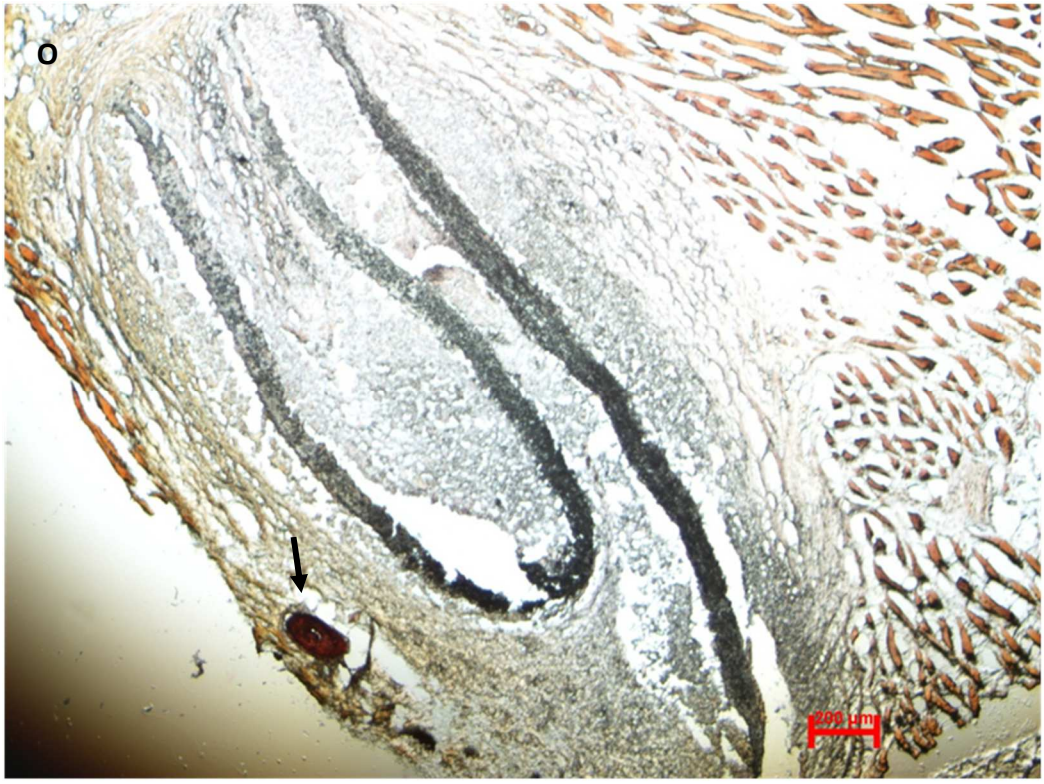


P
200 µm

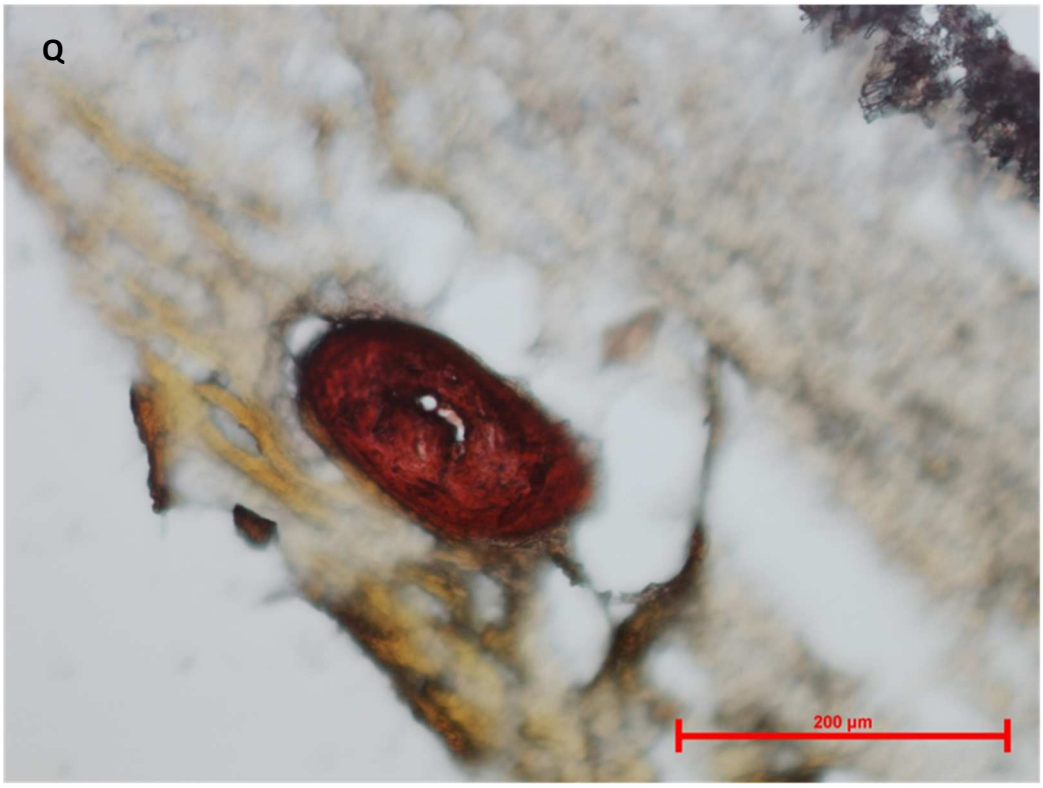
Q
200 µm

References

1. Service, R.F., *Tissue Engineers Build New Bone.* Science, 2000. **289**(5484): p. 1498-1500.

2. Dimitriou, R., et al., *Bone regeneration: current concepts and future directions.* BMC Medicine, 2011. **9**(1): p. 66.

3. Janicki, P. and G. Schmidmaier, *What should be the characteristics of the ideal bone graft substitute? Combining scaffolds with growth factors and/or stem cells.* Injury, 2011. **42**: p. S77-S81.

4. Hollister, S.J. and W.L. Murphy, *Scaffold Translation: Barriers Between Concept and Clinic.* Tissue Engineering Part B: Reviews, 2011. **17**(6): p. 459-474.

5. Rose, F.R.A.J. and R.O.C. Oreffo, *Bone Tissue Engineering: Hope vs Hype.* Biochemical and Biophysical Research Communications, 2002. **292**(1): p. 1-7.

6. Szpalski, C., et al., *Bone Tissue Engineering: Current Strategies and Techniques Part I-Scaffolds.* Tissue Engineering Part B: Reviews, 2011.

7. Kneser, U., et al., *Tissue engineering of bone: the reconstructive surgeon's point of view.* Journal of Cellular and Molecular Medicine, 2006. **10**(1): p. 7-19.

8. E.G Khaled, M.S., S Hindocha, M Griffin, Wasim S Khan, *Tissue Engineering for Bone Production- Stem Cells, Gene Therapy and Scaffolds.* Open Orthop J., 2011(5): p. 289-295.

9. Liu, X. and P.X. Ma, *Polymeric Scaffolds for Bone Tissue Engineering.* Annals of Biomedical Engineering, 2004. **32**(3): p. 477-486.

10. Bose, S., S. Vahabzadeh, and A. Bandyopadhyay, *Bone tissue engineering using 3D printing.* Materials Today, 2013. **16**(12): p. 496-504.

11. SCOTT P. BRUDER, K.H.K., VICTOR M. GOLDBERG, SUDHA KADIYALA, *The effect of implants loaded with autologous mesenchymal stem cells on the healing of canine segmental bone defects.* J Bone Joint Surg Am., 1998. **80**(7): p. 985-96.

12. Chistolini, P., et al., *Biomechanical evaluation of cell-loaded and cell-free hydroxyapatite implants for the reconstruction of segmental bone defects.* Journal of Materials Science: Materials in Medicine, 1999. **10**(12): p. 739-742.

13. Kon, E., et al., *Autologous bone marrow stromal cells loaded onto porous hydroxyapatite ceramic accelerate bone repair in critical-size defects of sheep long bones.* Journal of Biomedical Materials Research, 2000. **49**(3): p. 328-337.

14. Krebsbach, P.H., et al., *Repair of Craniotomy Defects Using Bone Marrow Stromal Cells.* Transplantation, 1998. **66**(10): p. 1272-1278.

15. Petite, H., et al., *Tissue-engineered bone regeneration.* Nat Biotech, 2000. **18**(9): p. 959-963.

16. Marcacci, M., et al., *Stem Cells Associated with Macroporous Bioceramics for Long Bone Repair: 6- to 7-Year Outcome of a Pilot Clinical Study.* Tissue Engineering, 2007. **13**(5): p. 947-955.

17. Quarto, R., et al., *Repair of Large Bone Defects with the Use of Autologous Bone Marrow Stromal Cells.* New England Journal of Medicine, 2001. **344**(5): p. 385-386.

18. Matsumoto, T., et al., *Therapeutic Potential of Vasculogenesis and Osteogenesis Promoted by Peripheral Blood CD34-Positive Cells for Functional Bone Healing.* The American Journal of Pathology, 2006. **169**(4): p. 1440-1457.

19. Zuk, P.A., et al., *Multilineage Cells from Human Adipose Tissue: Implications for Cell-Based Therapies.* Tissue Engineering, 2001. **7**(2): p. 211-228.

20. Jackson, W.M., et al., *Mesenchymal progenitor cells derived from traumatized human muscle.* Journal of Tissue Engineering and Regenerative Medicine, 2009. **3**(2): p. 129-138.

21. Marot, D., M. Knezevic, and G.V. Novakovic, *Bone tissue engineering with human stem cells.* Stem Cell Research & Therapy, 2010. **1**(2): p. 10-10.

22. Dimitriou, R., E. Tsiridis, and P.V. Giannoudis, *Current concepts of molecular aspects of bone healing.* Injury, 2005. **36**(12): p. 1392-1404.

23. Reddi, A., *Regulation of cartilage and bone differentiation by bone morphogenetic proteins.* Curr Opin Cell Biol, 1992. **4**(5): p. 850-5.

24. Argintar, E., S. Edwards, and J. Delahay, *Bone morphogenetic proteins in orthopaedic trauma surgery.* Injury, 2011. **42**(8): p. 730-734.

25. Fischer, J., et al., *Future of local bone regeneration – Protein versus gene therapy.* Journal of Cranio-Maxillofacial Surgery, 2011. **39**(1): p. 54-64.

26. Kumar, S. and S. Ponnazhagan, *Gene Therapy for Osteoinduction.* Current Gene Therapy, 2004. **4**(3): p. 287-296.

27. PONDER, K.P., *An Introduction to Molecular Medicine and Gene Therapy*, T.F. Kresina, Editor. 2000, Wiley. p. 77-112.

28. Tang, Y., et al., *Combination of bone tissue engineering and BMP-2 gene transfection promotes bone healing in osteoporotic rats.* Cell Biology International, 2008. **32**(9): p. 1150-1157.

29. Calori, G.M., et al., *Bone morphogenetic proteins and tissue engineering: future directions.* Injury, 2009. **40, Supplement 3**(0): p. S67-S76.

30. Lieberman, J.R., et al., *Regional gene therapy with a BMP-2-producing murine stromal cell line induces heterotopic and orthotopic bone formation in rodents.* Journal of Orthopaedic Research, 1998. **16**(3): p. 330-339.

31. Breitbart AS, G.D., *Gene-enhanced tissue engineering: applications for bone healing using cultured periosteal cells transduced retrovirally with the BMP-7 gene.* Ann Plast Surg, 1999. **42**(5): p. 488-95.

32. Kim, K., et al., *Incorporation and controlled release of a hydrophilic antibiotic using poly(lactide-co-glycolide)-based electrospun nanofibrous scaffolds.* Journal of Controlled Release, 2004. **98**(1): p. 47-56.

33. Luu, Y.K., et al., *Development of a nanostructured DNA delivery scaffold via electrospinning of PLGA and PLA–PEG block copolymers.* Journal of Controlled Release, 2003. **89**(2): p. 341-353.

34. Chiu, J.B., et al., *Functionalization of poly(L-lactide) nanofibrous scaffolds with bioactive collagen molecules.* Journal of Biomedical Materials Research Part A, 2007. **83A**(4): p. 1117-1127.

35. Kim, K., et al., *Control of degradation rate and hydrophilicity in electrospun non-woven poly(d,l-lactide) nanofiber scaffolds for biomedical applications.* Biomaterials, 2003. **24**(27): p. 4977-4985.

36. Di Martino, A., et al., *Electrospun scaffolds for bone tissue engineering.* Musculoskeletal Surgery, 2011. **95**(2): p. 69-80.

37. Chiu, J.B., *Investigation of Cell Behavior in PLLA-based, Nanofibrous Electrospun Scaffolds for Tissue Engineering*, in *Biomedical Engineering*. 2005, Stony Brook University.

38. Matthews, J.A., et al., *Electrospinning of Collagen Nanofibers.* Biomacromolecules, 2002. **3**(2): p. 232-238.

39. Toskas, G., et al., *Chitosan(PEO)/silica hybrid nanofibers as a potential biomaterial for bone regeneration.* Carbohydrate Polymers, 2013. **94**(2): p. 713-722.

40. Lai, G.-J., et al., *Composite chitosan/silk fibroin nanofibers for modulation of osteogenic differentiation and proliferation of human mesenchymal stem cells.* Carbohydrate Polymers, 2014. **111**(0): p. 288-297.

41. Ki, C., et al., *Development of 3-D nanofibrous fibroin scaffold with high porosity by electrospinning: implications for bone regeneration.* Biotechnology Letters, 2008. **30**(3): p. 405-410.

42. Yanagida, H., et al., *Preparation and in vitro/in vivo evaluations of dimpled poly(l-lactic acid) fibers mixed/coated with hydroxyapatite nanocrystals.* Journal of Artificial Organs, 2011. **14**(4): p. 331-341.

43. Lao, L., et al., *Poly(lactide-co-glycolide)/hydroxyapatite nanofibrous scaffolds fabricated by electrospinning for bone tissue engineering.* Journal of Materials Science: Materials in Medicine, 2011. **22**(8): p. 1873-1884.

44. Nguyen, T.-H., et al., *A novel fibrous scaffold composed of electrospun porous poly(ε-caprolactone) fibers for bone tissue engineering.* Journal of Biomaterials Applications, 2013. **28**(4): p. 514-528.

45. Cheng, Y., et al., *Collagen Functionalized Bioactive Nanofiber Matrices for Osteogenic Differentiation of Mesenchymal Stem Cells: Bone Tissue Engineering.* Journal of Biomedical Nanotechnology, 2014. **10**(2): p. 287-298.

46. Kim, B.S., et al., *Effect of nanofiber content on bone regeneration of silk fibroin/poly(ε-caprolactone) nano/microfibrous composite scaffolds.* International Journal of Nanomedicine, 2015. **10**: p. 485-502.

47. Balaji Raghavendran, H.R., et al., *A Comparative Study on In Vitro Osteogenic Priming Potential of Electron Spun Scaffold PLLA/HA/Col, PLLA/HA, and PLLA/Col for Tissue Engineering Application.* PLoS ONE, 2014. **9**(8): p. e104389.

48. Li, D., et al., *Enhanced Biocompatibility of PLGA Nanofibers with Gelatin/Nano-Hydroxyapatite Bone Biomimetics Incorporation.* ACS Applied Materials & Interfaces, 2014. **6**(12): p. 9402-9410.

49. Wang, J., et al., *Core-shell PLGA/collagen nanofibers loaded with recombinant FN/CDHs as bone tissue engineering scaffolds.* Connective Tissue Research, 2014. **55**(4): p. 292-298.

50. Haider, A., K.C. Gupta, and I.-K. Kang, *Morphological Effects of HA on the Cell Compatibility of Electrospun HA/PLGA Composite Nanofiber Scaffolds.* BioMed Research International, 2014. **2014**: p. 308306.

51. Barbanti, S.H., et al., *Porous and dense poly(L-lactic acid) and poly(D,L-lactic acid-co-glycolic acid) scaffolds: In vitro degradation in culture medium and osteoblasts*

culture. Journal of Materials Science: Materials in Medicine, 2004. **15**(12): p. 1315-1321.

52. Weir, N.A., et al., *Degradation of poly-L-lactide. Part 1: in vitro and in vivo physiological temperature degradation.* Proceedings of the Institution of Mechanical Engineers, Part H: Journal of Engineering in Medicine, 2004. **218**(5): p. 307-319.

53. Merolli, A., C. Gabbi, and A. Cacchioli, *Bone response to polymers based on poly-lactic acid and having different degradation times.* Journal of Materials Science: Materials in Medicine, 2001. **12**(9): p. 775-778.

54. Tsuji, H. and K. Ikarashi, *In vitro hydrolysis of poly(l-lactide) crystalline residues as extended-chain crystallites. Part I: long-term hydrolysis in phosphate-buffered solution at 37°C.* Biomaterials, 2004. **25**(24): p. 5449-5455.

55. Chen, C.-C., et al., *Preparation and characterization of biodegradable PLA polymeric blends.* Biomaterials, 2003. **24**(7): p. 1167-1173.

56. van Dijk, M., et al., *In vitro and in vivo degradation of bioabsorbable PLLA spinal fusion cages.* Journal of Biomedical Materials Research, 2002. **63**(6): p. 752-759.

57. Lu, L., et al., *In vitro degradation of porous poly(l-lactic acid) foams.* Biomaterials, 2000. **21**(15): p. 1595-1605.

58. Ikarashi, Y., et al., *Activation of Osteoblast-like MC3T3-E1 Cell Responses by Poly(Lactide).* Biological & Pharmaceutical Bulletin, 2000. **23**(12): p. 1470-1476.

59. Lee, B.N., et al., *In vivo biofunctionality comparison of different topographic PLLA scaffolds.* Journal of Biomedical Materials Research Part A, 2012. **100A**(7): p. 1751-1760.

60. Chen, L., et al., *Electrospun Poly(L-lactide)/Poly(<italic>ε</italic>-caprolactone) Blend Nanofibrous Scaffold: Characterization and Biocompatibility with Human Adipose-Derived Stem Cells.* PLoS ONE, 2013. **8**(8): p. e71265.

61. Andric, T., et al., *Fabrication and characterization of three-dimensional electrospun scaffolds for bone tissue engineering.* Journal of Biomedical Materials Research Part A, 2012. **100A**(8): p. 2097-2105.

62. Li, W.-J., et al., *Engineering controllable anisotropy in electrospun biodegradable nanofibrous scaffolds for musculoskeletal tissue engineering.* Journal of Biomechanics, 2007. **40**(8): p. 1686-1693.

63. Kern, B., et al., *Cbfa1 Contributes to the Osteoblast-specific Expression of type I collagen Genes.* Journal of Biological Chemistry, 2001. **276**(10): p. 7101-7107.

64. Giancotti, F.G. and E. Ruoslahti, *Integrin Signaling.* Science, 1999. **285**(5430): p. 1028-1033.

65. Zong, X., et al., *Structure and Morphology Changes during in Vitro Degradation of Electrospun Poly(glycolide-co-lactide) Nanofiber Membrane.* Biomacromolecules, 2003. **4**(2): p. 416-423.

66. Zhou, X., et al., *In vitro hydrolytic and enzymatic degradation of nestlike-patterned electrospun poly(D,L-lactide-co-glycolide) scaffolds.* Journal of Biomedical Materials Research Part A, 2010. **95A**(3): p. 755-765.

67. Lien, S.-M., L.-Y. Ko, and T.-J. Huang, *Effect of pore size on ECM secretion and cell growth in gelatin scaffold for articular cartilage tissue engineering.* Acta Biomaterialia, 2009. **5**(2): p. 670-679.

68. Oh, S.H., et al., *In vitro and in vivo characteristics of PCL scaffolds with pore size gradient fabricated by a centrifugation method.* Biomaterials, 2007. **28**(9): p. 1664-1671.

69. Tirabassi, R. *How to identify supercoils, nicks and circles in plasmid preps*. 2014; Available from: http://bitesizebio.com/13524/how-to-identify-supercoils-nicks-and-circles-in-plasmid-preps/.

70. Whited, B.M., et al., *Pre-osteoblast infiltration and differentiation in highly porous apatite-coated PLLA electrospun scaffolds.* Biomaterials, 2011. **32**(9): p. 2294-2304.

71. Gregory G. Reinholz, B.G., Larry Pederson, Emily S. Sanders, Malayannan Subramaniam, James N. Ingle, and Thomas C. Spelsberg, *Bisphosphonates directly regulate cell proliferation, differentiation, and gene expression in human osteoblasts.* Cancer Research, 2000. **60**(21): p. 6001-7.

72. King, W.J. and P.H. Krebsbach, *Growth factor delivery: How surface interactions modulate release in vitro and in vivo.* Advanced Drug Delivery Reviews, 2012. **64**(12): p. 1239-1256.

73. Wegman, F., et al., *Bone Morphogenetic Protein-2 Plasmid DNA as a Substitute for Bone Morphogenetic Protein-2 Protein in Bone Tissue Engineering.* Tissue Engineering Part A, 2013. **19**(23-24): p. 2686-2692.

74. Stanford, C.M., et al., *Rapidly Forming Apatitic Mineral in an Osteoblastic Cell Line (UMR 10601 BSP).* Journal of Biological Chemistry, 1995. **270**(16): p. 9420-9428.

75. Addison, W.N., et al., *Extracellular matrix mineralization in murine MC3T3-E1 osteoblast cultures: An ultrastructural, compositional and comparative analysis with mouse bone.* Bone, 2015. **71**(0): p. 244-256.

76. Tsuda, H., et al., *Enhanced osteoinduction by mesenchymal stem cells transfected with a fiber-mutant adenoviral BMP2 gene.* The Journal of Gene Medicine, 2005. **7**(10): p. 1322-1334.

77. Dong, H., et al., *Ectopic Osteogenesis by Ex Vivo Gene Therapy Using Beta Tricalcium Phosphate as a Carrier.* Connective Tissue Research, 2008. **49**(5): p. 343-350.

78. Brannen, T.A., *The Hind Limb Myology of the Laboratory Mouse, Mus Musculus: With Comparisons to Other Rodent Genera*. 1979: Kansas State University.

79. Burdick, J.A., et al., *An investigation of the cytotoxicity and histocompatibility of in situ forming lactic acid based orthopedic biomaterials.* Journal of Biomedical Materials Research, 2002. **63**(5): p. 484-491.

80. Barthel LK, R.P., *Improved method for obtaining 3-microns cryosections for immunocytochemistry.* J Histochem Cytochem, 1990. **38**(9): p. 1383-8.

81. Urist, M.R., *Bone: Formation by Autoinduction.* Science, 1965. **150**(3698): p. 893-899.

82. Urist, M., *The Classic: A Morphogenetic Matrix for Differentiation of Bone Tissue.* Clinical Orthopaedics and Related Research®, 2009. **467**(12): p. 3068-3070.

83. Urist, M.R. and B.S. Strates, *Bone Morphogenetic Protein.* Journal of Dental Research, 1971. **50**(6): p. 1392-1406.

84. Van de Putte KA, U.M., *Osteogenesis in the interior of intramuscular implants of decalcified bone matrix.* Clin Orthop Relat Res, 1965. **1965 Nov-Dec;43**: p. 257-70.

85. Simon, Z., et al., *Heterotopic Bone Formation Around Sintered Porous-Surfaced Ti-6Al-4V Implants Coated with Native Bone Morphogenetic Proteins.* Implant Dentistry, 2006. **15**(3): p. 265-274 10.1097/01.id.0000226754.71828.6b.

86. Si, X., Y. Jln, and L. Yang, *Induction of new bone by ceramic bovine bone with recombinant human bone morphogenetic protein 2 and transforming growth factor ß.* International Journal of Oral and Maxillofacial Surgery, 1998. **27**(4): p. 310-314.

87. Pekkarinen, T., et al., *Influence of ethylene oxide sterilization on the activity of native reindeer bone morphogenetic protein.* International Orthopaedics, 2004. **28**(2): p. 97-101.

88. T. Pekkarinen, T.S.L., O. Hietala, and P. Jalovaara, *New Bone Formation Induced by Injection of Native Reindeer Bone Morphogenetic Protein Extract.* Scandinavian Journal of Surgery, 2003. **92**(3): p. 227-230.

89. Musgrave, D.S., et al., *Adenovirus-mediated direct gene therapy with bone morphogenetic protein-2 produces bone.* Bone, 1999. **24**(6): p. 541-547.

90. Park, J., et al., *Bone regeneration in critical size defects by cell-mediated BMP-2 gene transfer: a comparison of adenoviral vectors and liposomes.* Gene Ther, 2003. **10**(13): p. 1089-1098.

91. Kobsa, S., et al., *An electrospun scaffold integrating nucleic acid delivery for treatment of full-thickness wounds.* Biomaterials, 2013. **34**(15): p. 3891-3901.

92. Mariko Kawai, K.B., Shinji Kaihara, Junya Sonobe, Kimimitsu Oda, Tadahiko Iizuka, and Hiroki Maruyama., *Ectopic Bone Formation by Human Bone Morphogenetic Protein-2 Gene Transfer to Skeletal Muscle Using Transcutaneous Electroporation.* Human Gene Therapy, 2003. **14**(16): p. 1547-1556.

93. Ono, I., et al., *Combination of porous hydroxyapatite and cationic liposomes as a vector for BMP-2 gene therapy.* Biomaterials, 2004. **25**(19): p. 4709-4718.

94. Park, J., et al., *The effect on bone regeneration of a liposomal vector to deliver BMP-2 gene to bone grafts in peri-implant bone defects.* Biomaterials, 2007. **28**(17): p. 2772-2782.

95. Lu, Z.-Z., et al., *Biodegradable polycation and plasmid DNA multilayer film for prolonged gene delivery to mouse osteoblasts.* Biomaterials, 2008. **29**(6): p. 733-741.

96. Jewell, C.M., et al., *Multilayered polyelectrolyte films promote the direct and localized delivery of DNA to cells.* Journal of Controlled Release, 2005. **106**(1–2): p. 214-223.

97. Sakai, S., et al., *Surface immobilization of poly(ethyleneimine) and plasmid DNA on electrospun poly(L-lactic acid) fibrous mats using a layer-by-layer approach for gene delivery.* Journal of Biomedical Materials Research Part A, 2009. **88A**(2): p. 281-287.

98. Carmel, C.A.K.-H.T.N.G.R.A.S.H.S.L.A., *Healing Bone Using RecombinantvHuman Bone Morphogenetic Protein 2 and Copolymer.* CLINICAL ORTHOPAEDICS AND RELATED RESEARCH, 1998. **349**(April): p. 205-217.

99. Avilés, M.O., et al., *The contribution of plasmid design and release to in vivo gene expression following delivery from cationic polymer modified scaffolds.* Biomaterials, 2010. **31**(6): p. 1140-1147.

100. Weiss, D., D. Liggitt, and J. Clark, *Histochemical Discrimination of Endogenous Mammalian β-galactosidase Activity from that Resulting from lac-Z Gene Expression.* The Histochemical Journal, 1999. **31**(4): p. 231-236.

101. Brazelton, T.R. and H.M. Blau, *Optimizing Techniques for Tracking Transplanted Stem Cells In Vivo.* STEM CELLS, 2005. **23**(9): p. 1251-1265.

102. H.-G. Kopp, A.T.H., S.V. Shmelkov, S. Rafii, *ß-Galactosidase staining on bone marrow. The osteoclast pitfall.* Histology and Histopathology, 2007(22): p. 971-976.

103. Rosen, V., *BMP2 signaling in bone development and repair.* Cytokine & Growth Factor Reviews, 2009. **20**(5–6): p. 475-480.

104. Bragdon, B., et al., *Bone Morphogenetic Proteins: A critical review.* Cellular Signalling, 2011. **23**(4): p. 609-620.

105. Lou, J., et al., *Involvement of ERK in BMP-2 Induced Osteoblastic Differentiation of Mesenchymal Progenitor Cell Line C3H10T1/2.* Biochemical and Biophysical Research Communications, 2000. **268**(3): p. 757-762.

106. Kyeong-Sook Lee, H.-J.K., Qing-Lin Li,1 Xin-Zi Chi, Chisato Ueta, Toshihisa Komori, John M. Wozney, Eung-Gook Kim, Je-Young Choi, Hyun-Mo Ryoo, Suk-Chul Bae, *Runx2 Is a Common Target of Transforming Growth Factor β1 and Bone Morphogenetic Protein 2, and Cooperation between Runx2 and Smad5 Induces Osteoblast-Specific Gene Expression in the Pluripotent Mesenchymal Precursor Cell Line C2C12.* Mol Cell Biol, 2000. **20**(23): p. 8783-8792.

107. Lee, M.-H., et al., *BMP-2-induced Runx2 Expression Is Mediated by Dlx5, and TGF-β1 Opposes the BMP-2-induced Osteoblast Differentiation by Suppression of Dlx5 Expression.* Journal of Biological Chemistry, 2003. **278**(36): p. 34387-34394.

108. Ducy, P., et al., *Osf2/Cbfa1: A Transcriptional Activator of Osteoblast Differentiation.* Cell, 1997. **89**(5): p. 747-754.

109. Gao, Y., et al., *Molecular cloning, structure, expression, and chromosomal localization of the human Osterix (SP7) gene.* Gene, 2004. **341**(0): p. 101-110.

110. Lian JB, H.P., Gallop PM, *Properties and biosynthesis of a vitamin K-dependent calcium binding protein in bone.* Fed Proc, 1978. **37**(12): p. 2615-20.

111. Wosczyna, M.N., et al., *Multipotent progenitors resident in the skeletal muscle interstitium exhibit robust BMP-dependent osteogenic activity and mediate heterotopic ossification.* Journal of Bone and Mineral Research, 2012. **27**(5): p. 1004-1017.

112. Carragee, E.J., E.L. Hurwitz, and B.K. Weiner, *A critical review of recombinant human bone morphogenetic protein-2 trials in spinal surgery: emerging safety concerns and lessons learned.* The Spine Journal, 2011. **11**(6): p. 471-491.